Available online at http://scik.org
J. Math. Comput. Sci. 11 (2021), No. 3, 3663-3728
https://doi.org/10.28919/jmcs/5692
ISSN: 1927-5307

A COMPREHENSIVE REVIEW OF DATASETS FOR STATISTICAL RESEARCH IN PROBABILITY AND QUALITY CONTROL

MUHAMMAD Z. ARSHAD[1,*], MUHAMMAD Z. IQBAL[1], ALYA AL MUTAIRI[2]

[1]Department of Mathematics and Statistics, University of Agriculture, Faisalabad, Pakistan

[2]Department of Mathematics, Faculty of Science, Taibah University, Medina, Saudi Arabia

Abstract: This paper aims to promote the utility of datasets and to facilitate the practitioners of applied, theoretical as well as research scholars, whose research work is suffering owing to the unavailability of data. For this, we develop a list of one hundred and eleven; most cited datasets are classified in such an organized way under one roof so that it might be helpful. Accordingly, we have pursued the International Impact Factor and Peer-Reviewed journals and books to acquire the multidisciplinary univariate continuous real-time datasets. All the datasets are systematized according to the following characters such as (i) $(0, \infty)$, $(0, 1)$, $(-\infty, \infty)$, and (ii) left-skewed, right-skewed, symmetric, bath-tub, bi-modal, and tri-modal shapes. However, this comprehensive paper will provide a solid foundation to the practitioners and researchers and they may continue their research work for the betterment of this world.

Keywords: dataset; probability distribution; quality control; hydrology; medical science; metrology; automobile; aviation; textile; agriculture; engineering; geology; insurance; climatology; antinarcotics; communication; highway; commerce.

2010 AMS Subject Classification: Primary 62F15, Secondary 65C20.

[*]Corresponding author
E-mail address: profarshad@yahoo.com
Received March 13, 2021

1. INTRODUCTION

Over the past few decades, the collection of data and its handling was considered a big issue and certainly, this statement is true so far. Most of the time, it is to be observed that the practitioners and research scholars seem to be worried about the data they are required for investigation. Sometimes, researchers feel that they can obtain the data without any difficulty, and sometimes, it is not accessible. One of the big issues not to access the data is the limited resources of the poor researcher that actively participates and agitates the whole research work. In addition, most of the international impact factor and peer-reviewed journals and books demand to pay a huge amount in terms of dollars to download the articles but we are incapable to do so. This comprehensive review of datasets is designed in such a way to facilitate, improve the understanding and readability of the readers. For this, each dataset has been presented by two graphics including histogram and total test time curve (TTT curve proposed by [1]. Various forms of the TTT-plot may have and one may interpret likewise: If the curve approaches a straight diagonal function, the constant failure rate is adequate. When the curve is convex or concave, the failure rate function is monotonically increasing or decreasing respectively, is adequate. If the failure rate function is convex and concave, the failure rate function in format U (bath-tub) is adequate, otherwise, the failure rate function uni-modal is more appropriate. Further, the sources of data collection are properly cited therein. Several useful links are also mentioned at the end of this list. At last, we would like to share one thing that all the data sets are handled very carefully. For a comprehensive review of datasets, we encourage the readers to see the following.

1- The following bathtub shaped data presents a bat-tub shaped failure rate, discussed by [1], consists of times to first failure of fifty devices and the values are:

0.1, 0.2, 1.0, 1.0, 1.0, 1.0, 1.0, 2.0, 3.0, 6.0, 7.0, 11.0, 12.0, 18.0, 18.0, 18.0, 18.0, 18.0, 21.0, 32.0, 36.0, 40.0, 45.0, 45.0, 47.0, 50.0, 55.0, 60.0, 63.0, 63.0, 67.0, 67.0, 67.0, 67.0, 72.0, 75.0, 79.0, 82.0, 82.0, 83.0, 84.0, 84.0, 84.0, 85.0, 85.0, 85.0, 85.0, 85.0, 86.0, 86.0.

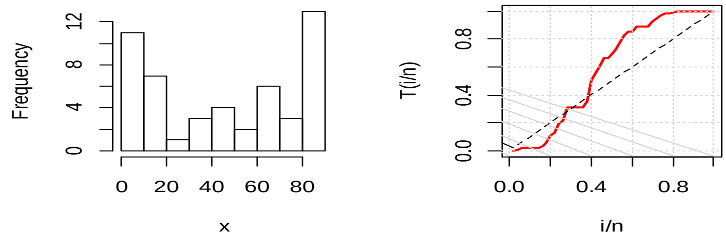

Figure 1. The extreme nature of the bathtub shaped failure rate

2- The following right-skewed data presents the exceedances of flood peaks (in m3/s) of the Wheaton River near Carcross in Yukon Territory, Canada. The data consist of 72 exceedances for the years 1958–1984, rounded to one decimal place. This data was analyzed by [2] and is given as follow:

1.7, 2.2, 14.4, 1.1, 0.4, 20.6, 5.3, 0.7, 1.9, 13, 12, 9.3, 1.4, 18.7, 8.5, 25.5, 11.6, 14.1, 22.1, 1.1, 2.5, 14.4, 1.7, 37.6, 0.6, 2.2, 39, 0.3, 15, 11, 7.3, 22.9, 0.1, 1.7, 1.1, 0.6, 9, 1.7, 7, 20.1, 0.4, 2.8, 14.1, 9.9, 10.4, 10.7, 30, 3.6, 5.6, 30.8, 13.3, 4.2, 25.5, 3.4, 11.9, 21.5, 27.6, 36.4, 2.7, 64, 1.5, 2.5, 27.4, 1, 27.1, 20.2, 16.8, 5.3, 9.7, 27.5, 2.5, 27.

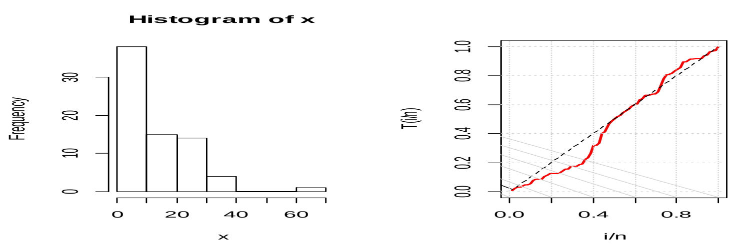

Figure 2. The right-skewed data of flood peaks of the Wheaton River in Yukon Territory, Canada

3- This following right-skewed data set discussed by [3], presents the maximum annual flood discharges of the North Saskatchewan in units of 1000 cubic feet per second, of the north Saskatchewan river at Edmonton, over a period of 47 years. The data is:

19.885, 20.940, 21.820, 23.700, 24.888, 25.460, 25.760, 26.720, 27.500, 28.100, 28.600, 30.200, 30.380, 31.500, 32.600, 32.680, 34.400, 35.347, 35.700, 38.100, 39.020, 39.200, 40.000, 40.400, 40.400, 42.250, 44.020, 44.730, 44.900, 46.300, 50.330, 51.442, 57.220, 58.700, 58.800, 61.200, 61.740, 65.440, 65.597, 66.000, 74.100, 75.800, 84.100, 106.600, 109.700, 121.970, 121.970, 185.560.

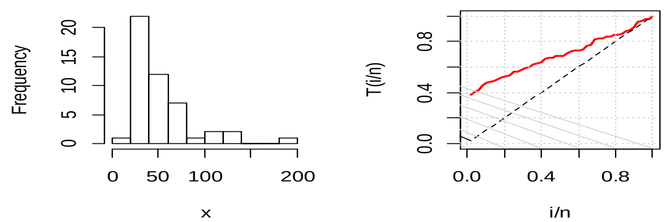

Figure 3. The maximum annual flood discharges of the North Saskatchewan

4- The following right skewed data, developed by [4], for 47 years of Styx River (Jeogla) about annual maximum flood peaks series are analyzed. The values of data are:

878, 541, 521, 513, 436, 411, 405, 315, 309, 300, 294, 258, 255, 235, 221, 220, 206, 196, 194, 190, 186, 177, 164, 126, 117, 111, 108, 105, 92.2, 88.6, 79.9, 74, 71.9, 62.6, 61.2, 60.3, 58, 53.5, 39.1, 26.7, 26.1, 23.8, 22.4, 22.1, 18.6, 13, 8.18.

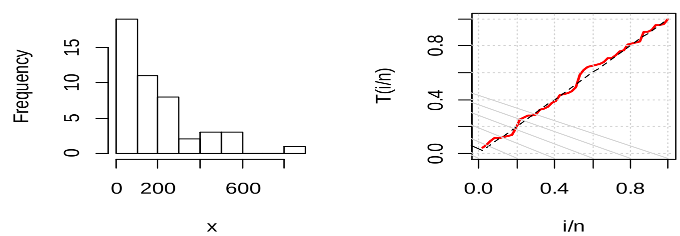

Figure 4. The right-skewed data for 47 years of Styx River about annual maximum flood peaks series

5- The following right skewed data, discussed by [5], comprises 59 annual maximum precipitations in Karachi city, Pakistan for the years 1950-2009. The precipitation records are necessary for water management studies and flood defense systems. The precipitation data is used to predict the flood and drought. The precipitation data also help to minimize the risk of large hydraulic structures. The values of data are:

117.6, 157.7, 148.6, 11.4, 5.6, 63.6, 62.4, 11.8, 6.5, 54.9, 39.9, 16.8, 30.2, 38.4, 76.9, 73.4, 85, 256.3, 24.9, 148.6, 160.5, 131.3, 77, 155.2, 217.2, 105.5, 166.8, 157.9, 73.6, 291.4, 210.3, 315.7, 107.7, 33.3, 302.6, 159.1, 78.7, 33.2, 52.2, 92.7,150.4, 43.7, 68.3, 20.8, 179.4, 245.7, 19.5, 30, 270.4, 160, 96.3, 185.7, 429.3, 184.9, 262.5, 80.6, 138.2, 28, 39.3.

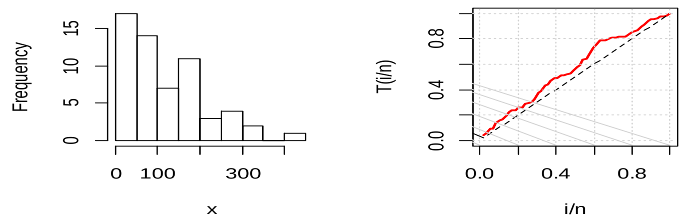

Figure 5. Comprises 59 annual maximum precipitations in Karachi city, Pakistan

6- The following extreme right skewed data set, developed by [6], consists of 40 losses that occurred in 1977 due to wind-related catastrophes, and the observations are:

2, 2, 2, 2, 2, 2, 2, 2, 2, 2, 2, 2, 3, 3, 3, 4, 4, 4, 5, 5, 5, 6, 6, 6, 6, 8, 8, 9, 15, 17, 22, 23, 24, 24, 25, 27, 3243.

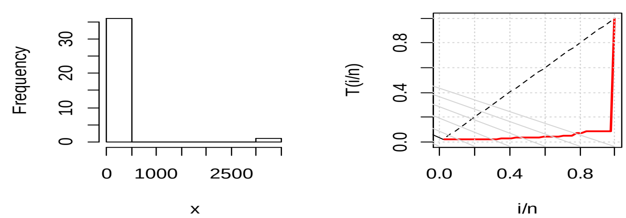

Figure 6. The 40 losses that occurred in 1977 due to wind-related catastrophes

7- The following right-skewed data set, discussed by [7], consists of failure times or censoring times for 36 appliances subjected to an automated life test. Failures are mainly classified into 18 different modes, though among 33 observed failures only 7 modes are presented and only models 6 and 9 appear more than once. We are mainly interested in failure mode 9. The data is given below:

1167, 1925, 1990, 2223, 2400, 2471, 2551, 2568, 2694, 3034, 3112, 3214, 3478, 3504, 4329, 6976, 7846.

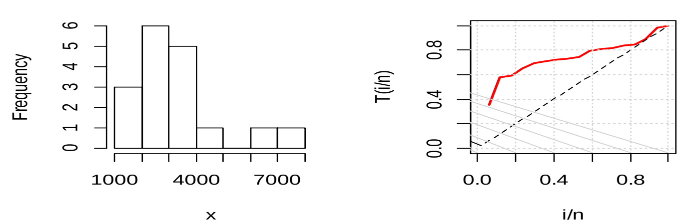

Figure 7. Failure times or censoring times for 36 appliances subjected to an automated life test

8- The following skewed to right data developed by [7], is the number of million revolutions before failure for each of the 23 ball bearings in the life tests and it is given:

17.88, 28.92, 33.0, 41.52, 42.12, 45.6, 48.8, 51.84, 51.96, 54.12, 55.56, 67.8, 68.44, 68.88, 84.12, 93.12, 98.64, 105.12, 105.84, 105.84, 127.92, 128.04, 173.4.

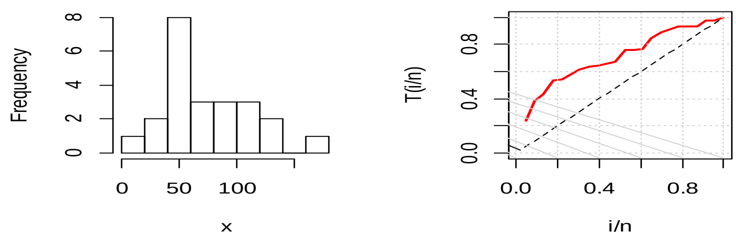

Figure 8. The skewed to right data of the number of million revolutions

9- The following extreme natured (skewed to right) a set of data projected by [7], presents the 36 appliances failure times subjected to an automatic life test and the values are:

11, 35, 49, 170, 329, 381, 708, 958, 1062, 1167, 1594, 1925, 1990, 2223, 2327, 2400, 2451, 2471, 2551, 2565, 2568, 2694, 2702, 2761, 2831, 3034, 3059, 3112, 3214, 3478, 3504, 4329, 6367, 6976, 7846, 13403.

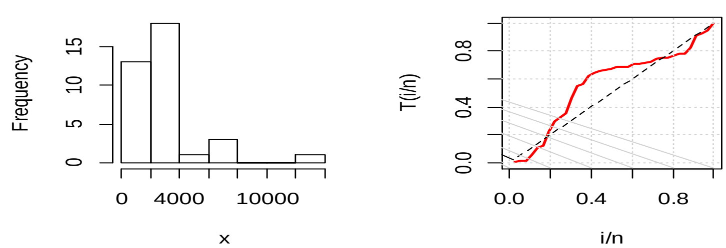

Figure 9. The skewed to right of the 36 appliances failure times subjected to an automatic life test

10- The following censored (in Gba) values about the breaking stress of carbon fibers discussed by [8], present almost the symmetric trend of data and the values are:

3.70, 2.74, 2.73, 2.50, 3.60, 3.11, 3.27, 2.87, 1.47, 3.11, 3.56, 4.42, 2.41, 3.19, 3.22, 1.69, 3.28, 3.09, 1.87, 3.15, 4.90, 1.57, 2.67, 2.93, 3.22, 3.39, 2.81, 4.20, 3.33, 2.55, 3.31, 3.31, 2.85, 1.25, 4.38, 1.84, 0.39, 3.68, 2.48, 0.85, 1.61, 2.79, 4.70, 2.03, 1.89, 2.88, 2.82, 2.05, 3.65, 3.75, 2.43, 2.95, 2.97, 3.39, 2.96, 2.35, 2.55, 2.59, 2.03, 1.61, 2.12, 3.15, 1.08, 2.56, 1.80, 2.53.

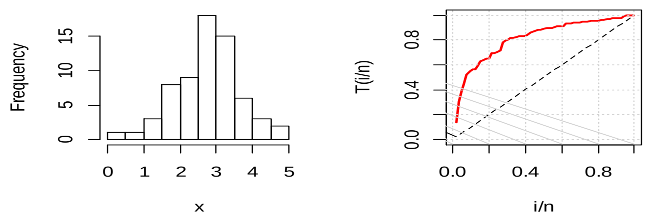

Figure 10. The symmetric trend values of the breaking stress of carbon fibers

11- The following data represents the symmetric behavior of the tensile strength about 100 observations of carbon fibers, discussed by [8], and the observations are:

3.7, 3.11, 4.42, 3.28, 3.75, 2.96, 3.39, 3.31, 3.15, 2.81, 1.41, 2.76, 3.19, 1.59, 2.17, 3.51, 1.84, 1.61, 1.57, 1.89, 2.74, 3.27, 2.41, 3.09, 2.43, 2.53, 2.81, 3.31, 2.35, 2.77, 2.68, 4.91, 1.57, 2.00, 1.17, 2.17, 0.39, 2.79, 1.08, 2.88, 2.73, 2.87, 3.19, 1.87, 2.95, 2.67, 4.20, 2.85, 2.55, 2.17, 2.97, 3.68, 0.81, 1.22, 5.08, 1.69, 3.68, 4.70, 2.03, 2.82, 2.50, 1.47, 3.22, 3.15, 2.97, 1.61, 2.05, 3.60, 3.11, 1.69, 4.90, 3.39, 3.22, 2.55, 3.56, 2.38, 1.92, 0.98, 1.59, 1.73, 1.71, 1.18, 4.38, 0.85, 1.80, 2.12, 3.65.

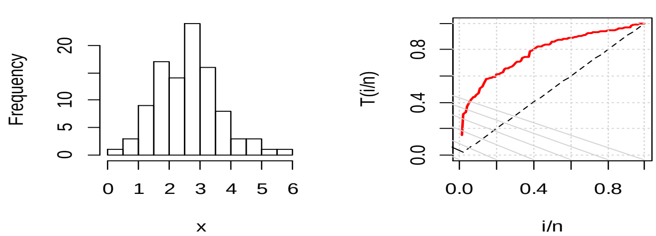

Figure 11. The symmetric behavior of the tensile strength of carbon fibers

12- The following symetircal dataset discussed by [8], is the strengths of 1.5 cm glass fibers and the values are:

0.39, 0.85, 1.08, 1.25, 1.47, 1.57, 1.61, 1.61, 1.69, 1.80, 1.84, 1.87, 1.89, 2.03, 2.03, 2.05, 2.12, 2.35, 2.41, 2.43, 2.48, 2.50, 2.53, 2.55, 2.55, 2.56, 2.59, 2.67, 2.73, 2.74, 2.79, 2.81, 2.82, 2.85, 2.87, 2.88, 2.93, 2.95, 2.96, 2.97, 3.09, 3.11, 3.11, 3.15, 3.15, 3.19, 3.22, 3.22, 3.27, 3.28, 3.31, 3.31, 3.33, 3.39, 3.39, 3.56, 3.60, 3.65, 3.68, 3.70, 3.75, 4.20, 4.38, 4.42, 4.70, 4.90.

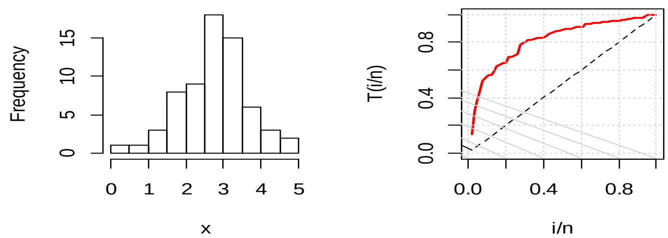

Figure 12. The symetircal strengths of 1.5 cm glass fibers

13- The following slightly left skewed dataset is the strengths of 1.5 cm glass fibers, discussed by [9], and the observations are:

0.55, 0.93, 1.25, 1.36, 1.49, 1.52, 1.58, 1.61, 1.64, 1.68, 1.73, 1.81, 2, 0.74, 1.04, 1.27, 1.39, 1.49, 1.53, 1.59, 1.61, 1.66, 1.68, 1.76, 1.82, 2.01, 0.77, 1.11, 1.28, 1.42, 1.5, 1.54, 1.6, 1.62, 1.66, 1.69, 1.76, 1.84, 2.24, 0.81, 1.13, 1.29, 1.48, 1.5, 1.55, 1.61, 1.62, 1.66, 1.7, 1.77, 1.84, 0.84, 1.24, 1.3, 1.48, 1.51, 1.55, 1.61, 1.63, 1.67, 1.7, 1.78, 1.89.

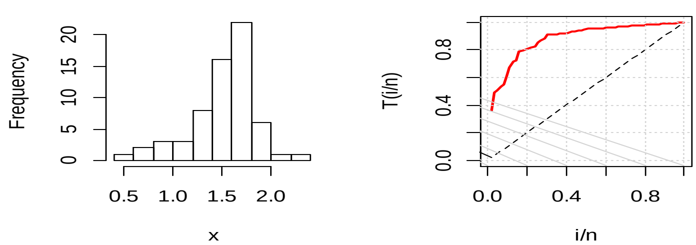

Figure 13. The slightly left skewed strengths of 1.5 cm glass fibers

14- The following extremely right skewed uncensored data set corresponding to remission times (in months) of bladder cancer 128 patients, discussed by [10], is given:

0.08, 2.09, 3.48, 4.87, 6.94, 8.66, 13.11, 23.63, 0.2, 2.23, 0.52, 4.98, 6.97, 9.02, 13.29, 0.4, 2.26, 3.57, 5.06, 7.09, 0.22, 13.8, 25.74, 0.5, 2.46, 3.46, 5.09, 7.26, 9.47, 14.24, 0.82, 0.51, 2.54, 3.7, 5.17, 7.28, 9.74, 14.76, 26.31, 0.81, 0.62, 3.28, 5.32, 7.32, 10.06, 14.77, 32.15, 2.64, 3.88, 5.32, 0.39, 10.34, 14.38, 34.26, 0.9, 2.69, 4.18, 5.34, 7.59, 10.66, 0.96, 36.66, 1.05, 2.69, 4.23, 5.41, 7.62, 10.75, 16.62, 43.01, 0.19, 2.75, 4.26, 5.41, 7.63, 17.12, 46.12, 1.26, 2.83, 4.33, 0.66, 11.25, 17.14, 79.05, 1.35, 2.87, 5.62, 7.87, 11.64, 17.36, 0.4, 3.02, 4.34, 5.71, 7.93, 11.79, 18.1, 1.46, 4.4, 5.85, 0.26, 11.98, 19.13, 1.76, 3.25, 4.5, 6.25, 8.37, 12.02, 2.02, 0.31, 4.51, 6.54, 8.53, 12.03, 20.28, 2.02, 3.36, 6.76, 12.07, 0.73, 2.07, 3.36, 6.39, 8.65, 12.63, 22.69, 5.49.

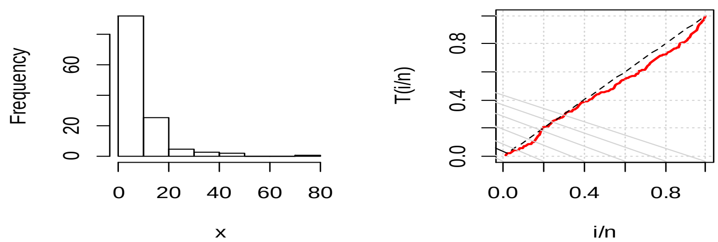

Figure 14. The remission times of bladder cancer 128 patients

15- This moderate skewed to left data set D2 consists of lifetimes of 43 blood cancer patients (in days) from one of the health hospitals in Saudi Arabia. The following data discussed by [11] and the observations are:

115, 181, 255, 418, 441, 461, 516, 739, 743, 789, 807, 865, 924, 983, 1025, 1062, 1063, 1165, 1191, 1222, 1222, 1251, 1277, 1290, 1357, 1369, 1408, 1455, 1478, 1519, 1578, 1578, 1599, 1603, 1605, 1696, 1735, 1799, 1815 ,1852, 1899, 1925, 1965.

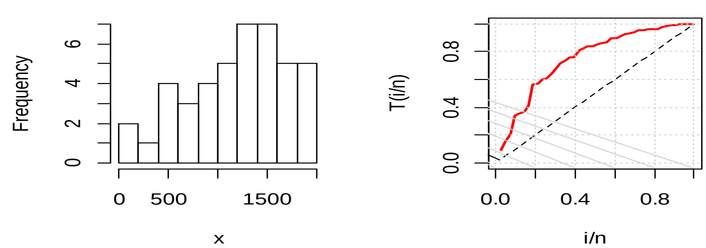

Figure 15. The lifetimes of 43 blood cancer patients from one of the health hospitals

16- The following symmetric set of data is the survival times (in months) of 20 acute myeloid leukemia patients discussed by [12], and the observations are:

2.226, 2.113, 3.631, 2.473, 2.720, 2.050, 2.061, 3.915, 0.871, 1.548, 2.746, 1.972, 2.265, 1.200, 2.967, 2.808, 1.079, 2.353, 0.726, 1.958.

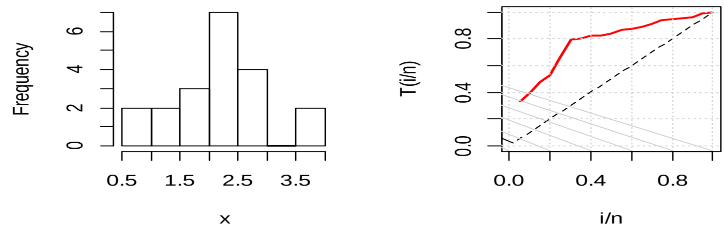

Figure 16. The survival times of 20 acute myeloid leukemia patients

17- The following data discussed by [13], skewed to right, present the survival times of one hundred and twenty-one (121) patients with breast cancer obtained from a large hospital in a period from 1929 to 1938.

0.3, 0.3, 4.0, 5.0, 5.6, 6.2, 6.3, 6.6, 6.8, 7.4, 7.5, 8.4, 8.4, 10.3, 11.0, 11.8, 12.2, 12.3, 13.5, 14.4, 14.4, 14.8, 15.5, 15.7, 16.2, 16.3, 16.5, 16.8, 17.2, 17.3, 17.5, 17.9, 19.8, 20.4, 20.9, 21.0, 21.0, 21.1, 23.0, 23.4, 23.6, 24.0, 24.0, 27.9, 28.2, 29.1, 30.0, 31.0, 31.0, 32.0, 35.0, 35.0, 37.0, 37.0, 37.0, 38.0, 38.0, 38.0, 39.0, 39.0, 40.0, 40.0, 40.0, 41.0, 41.0, 41.0, 42.0, 43.0, 43.0, 43.0, 44.0, 45.0, 45.0, 46.0, 46.0, 47.0, 48.0, 49.0, 51.0, 51.0, 51.0, 52.0, 54.0, 55.0, 56.0, 57.0, 58.0, 59.0, 60.0, 60.0, 60.0, 61.0, 62.0, 65.0, 65.0, 67.0, 67.0, 68.0, 69.0, 78.0, 80.0, 83.0, 88.0, 89.0, 90.0, 93.0, 96.0, 103.0, 105.0, 109.0, 109.0, 111.0, 115.0, 117.0, 125.0, 126.0, 127.0, 129.0, 129.0, 139.0, 154.0.

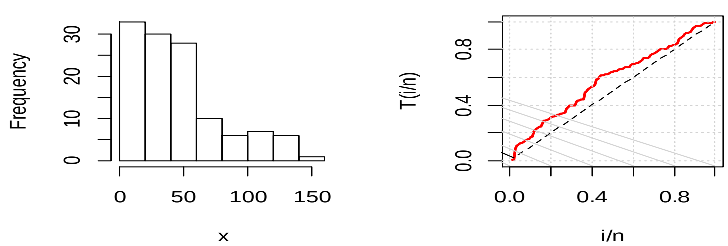

Figure 17. The survival times of one 121 patients with breast cancer

18- The following lifetime data indicates the right-skewed trend, originally reported by [14], studies the anxiety performed by a group of 166 normal women, i.e., outside of a pathological clinical picture (Townsville, Queensland, Australia)

0.01, 0.17, 0.01, 0.05, 0.09, 0.41, 0.05, 0.01, 0.13, 0.01, 0.05, 0.17, 0.01, 0.09, 0.01, 0.05, 0.09, 0.09, 0.05, 0.01, 0.01, 0.01, 0.29, 0.01, 0.01, 0.01, 0.01, 0.01, 0.01, 0.01, 0.01, 0.09, 0.37, 0.05, 0.01, 0.05, 0.29, 0.09, 0.01, 0.25, 0.01, 0.09, 0.01, 0.05, 0.21, 0.01, 0.01, 0.01, 0.13, 0.17, 0.37, 0.01, 0.01, 0.09, 0.57, 0.01, 0.01, 0.13, 0.05, 0.01, 0.01, 0.01, 0.01, 0.09, 0.13, 0.01, 0.01, 0.09, 0.09, 0.37, 0.01, 0.05, 0.01, 0.01, 0.13, 0.01, 0.57, 0.01, 0.01, 0.09, 0.01, 0.01, 0.01, 0.01, 0.01, 0.01, 0.05, 0.01, 0.01, 0.01, 0.13, 0.01, 0.25, 0.01, 0.01, 0.09, 0.13, 0.01, 0.01, 0.05, 0.13, 0.01, 0.09, 0.01, 0.05, 0.01, 0.05, 0.01, 0.09, 0.01, 0.37, 0.25, 0.05, 0.05, 0.25, 0.05, 0.05, 0.01, 0.05, 0.01, 0.01, 0.01, 0.17, 0.29, 0.57, 0.01, 0.05, 0.01, 0.09, 0.01, 0.09, 0.49, 0.45, 0.01, 0.01, 0.01, 0.05, 0.01, 0.17, 0.01, 0.13, 0.01, 0.21, 0.13, 0.01, 0.01, 0.17, 0.01, 0.01, 0.21, 0.13, 0.69, 0.25, 0.01, 0.01, 0.09, 0.13, 0.01, 0.05, 0.01, 0.01, 0.29, 0.25, 0.49, 0.01, 0.01.

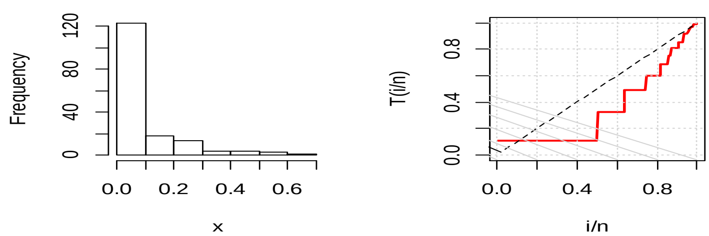

Figure 18. The lifetime of the right skewed trend in anxiety of normal women

19- The following data relates to the flood data with 20 observations, discussed by [15], present the skewed to right trend and the values are:

0.265, 0.269, 0.297, 0.315, 0.3235, 0.338, 0.379, 0.379, 0.392, 0.402, 0.412, 0.416, 0.418, 0.423, 0.449, 0.484, 0.494, 0.613, 0.654, 0.74.

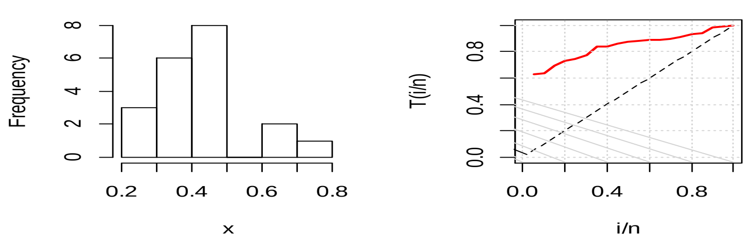

Figure 19. The skewed to right trend and the values to the Flood data

20- The following data set presented by [16], displays the skewed symmetric trend of data. This data discusses the total milk production in the first birth of 107 cows from the SINDI race. These cows are property of the Carnaúba farm which belongs to the Agropecuária Manoel Dantas Ltda (AMDA), located in Taperoá City, Paraíba (Brazil). The data is:

0.4365, 0.4260, 0.5140, 0.6907, 0.7471, 0.2605, 0.6196, 0.8781, 0.4990, 0.6058, 0.6891, 0.5770, 0.5394, 0.1479, 0.2356, 0.6012, 0.1525, 0.5483, 0.6927, 0.7261, 0.3323, 0.0671, 0.2361, 0.4800, 0.5707, 0.7131, 0.5853, 0.6768, 0.5350, 0.4151, 0.6789, 0.4576, 0.3259, 0.2303, 0.7687, 0.4371, 0.3383, 0.6114, 0.3480, 0.4564, 0.7804, 0.3406, 0.4823, 0.5912, 0.5744, 0.5481, 0.1131, 0.7290, 0.0168, 0.5529, 0.4530, 0.3891, 0.4752, 0.3134, 0.3175, 0.1167, 0.6750, 0.5113, 0.5447, 0.4143, 0.5627, 0.5150, 0.0776, 0.3945, 0.4553, 0.4470, 0.5285, 0.5232, 0.6465, 0.0650, 0.8492, 0.8147, 0.3627, 0.3906, 0.4438, 0.4612, 0.3188, 0.2160, 0.6707, 0.6220, 0.5629, 0.4675, 0.6844, 0.3413, 0.4332, 0.0854, 0.3821, 0.4694, 0.3635, 0.4111, 0.5349, 0.3751, 0.1546, 0.4517, 0.2681, 0.4049, 0.5553, 0.5878, 0.4741, 0.3598, 0.7629, 0.5941, 0.6174, 0.6860, 0.0609, 0.6488, 0.2747.

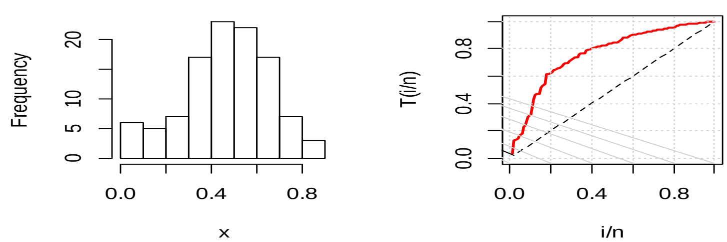

Figure 20. The skewed symmetric trend of the total milk production

21- The following data presents the extreme right to skewed behavior, study the failure times of 20 mechanical components, discussed by [17]. The values are:

0.067, 0.068, 0.076, 0.081, 0.084, 0.085, 0.085, 0.086, 0.089, 0.098, 0.098, 0.114, 0.114, 0.115, 0.121, 0.125, 0.131, 0.149, 0.160, 0.485.

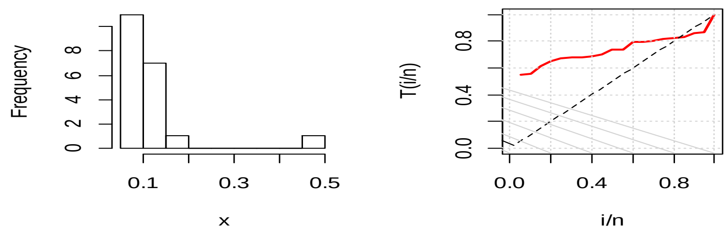

Figure 21. The extreme right to skewed behavior

22- The following symmetric data, discussed by [17], studies the failure times of windshields and the values are:

0.04, 0.3, 0.31, 0.557, 0.943, 1.07, 1.124, 1.248, 1.281, 1.281, 1.303, 1.432, 1.48, 1.51, 1.51, 1.568, 1.615, 1.619, 1.652, 1.652, 1.757, 1.795, 1.866, 1.876, 1.899, 1.911, 1.912, 1.9141, 0.981, 2.010, 2.038, 2.085, 2.089, 2.097, 2.135, 2.154, 2.190, 2.194, 2.223, 2.224, 2.23, 2.3, 2.324, 2.349, 2.385, 2.481, 2.610, 2.625, 2.632, 2.646, 2.661, 2.688, 2.823, 2.89, 2.9, 2.934, 2.962, 2.964, 3, 3.1, 3.114, 3.117, 3.166, 3.344, 3.376, 3.385, 3.443, 3.467, 3.478, 3.578, 3.595, 3.699, 3.779, 3.924, 4.035, 4.121, 4.167, 4.240, 4.255, 4.278, 4.305, 4.376, 4.449, 4.485, 4.570, 4.602, 4.663, 4.694.

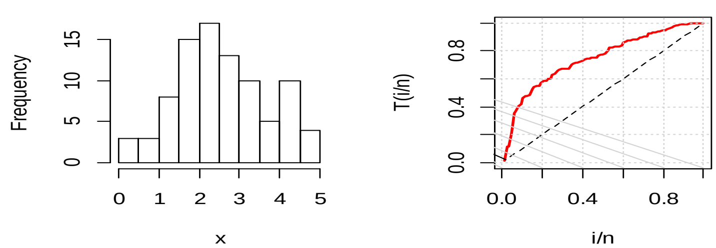

Figure 22. The symmetric of the failure times of windshields and the values

23- The following extreme skewed to right data, discussed by [17], presents the failure times of 50 components and the observations are:

0.036, 0.058, 0.061, 0.074, 0.078, 0.086, 0.102, 0.103, 0.114, 0.116, 0.148, 0.183, 0.192, 0.254, 0.262, 0.379, 0.381, 0.538, 0.570, 0.574, 0.590, 0.618, 0.645, 0.961, 1.228, 1.600, 2.006, 2.054, 2.804, 3.058, 3.076, 3.147, 3.625, 3.704, 3.931, 4.073, 4.393, 4.534, 4.893, 6.274, 6.816, 7.896, 7.904, 8.022, 9.337, 10.940, 11.020, 13.880, 14.730, 15.080.

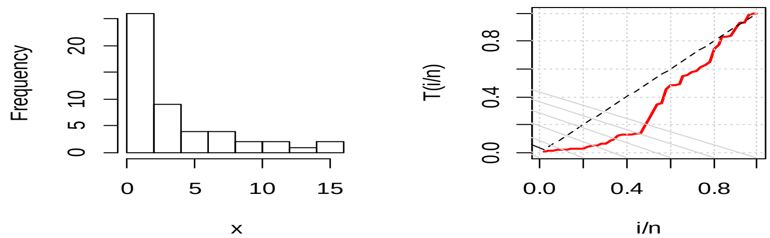

Figure 23. The extreme skewed to right of the failure times of 50 components and the observations

24- The following skewed to right, a complete data, discussed by [17], presents the failure times of 24 mechanical components. The observations are:

30.94, 18.51, 16.62, 51.56, 22.85, 22.38, 19.08, 49.56, 17.12, 10.67, 25.43, 10.24, 27.47, 14.70, 14.10, 29.93, 27.98, 36.02, 19.40, 14.97, 22.57, 12.26, 18.14, 18.84.

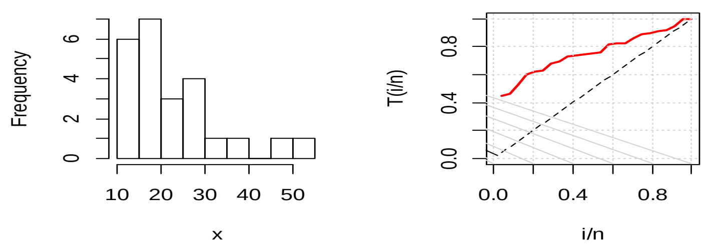

Figure 24. The skewed to the right of the failure times of 24 mechanical components

25- A censored set of data, discussed by [17], presents bi-modal behavior of data, for 30 items, are tested with test stopped after the 20-th hour failure (failure times of data is given). The values are:

2.45, 3.74, 3.92, 4.99, 6.73, 7.52, 7.73, 7.85, 7.94, 8.25, 8.37, 9.75, 10.86, 11.17, 11.37, 11.60, 11.96, 12.20, 13.24, 13.50.

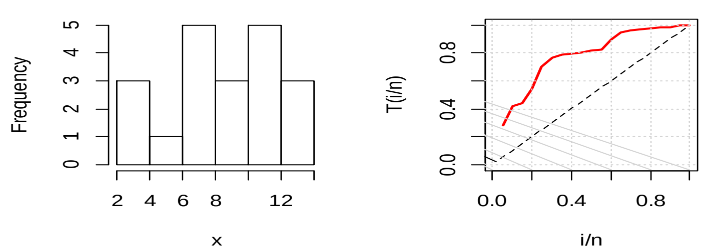

Figure 25. A bi-modal behavior after the 20-th hour failure

26- A skewed symmetric set of censored data, discussed by [17], contains 50 items that is tested and test is stopped after the 12-th hour. The failure times of data is given and the observations are:

0.80, 1.26, 1.29, 1.85, 2.41, 2.47, 2.76, 3.35, 3.68, 4.46, 4.65, 4.83, 5.21, 5.26, 5.36, 5.39, 5.53, 5.64, 5.80, 6.08, 6.38, 7.02, 7.18, 7.60, 8.13,8.46, 8.69, 10.52, 11.25, 11.90.

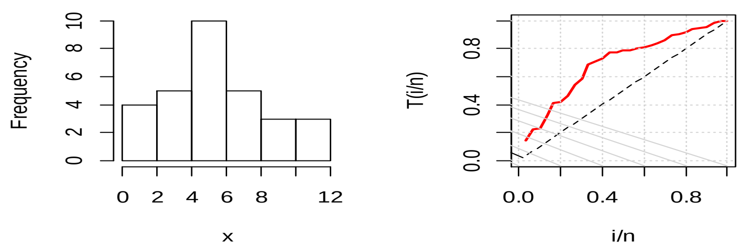

Figure 26. The skewed symmetric set of 50 items after the 12-th hour

27- A complete set of skewed to right data, discussed by [17], in which 20 items are tested till failure are discussed and the values are:

11.24, 1.92, 12.74, 22.48, 9.60, 11.50, 8.86, 7.75, 5.73, 9.37, 30.42, 9.17, 10.20, 5.52, 5.85, 38.14, 2.99, 16.58, 18.92, 13.36.

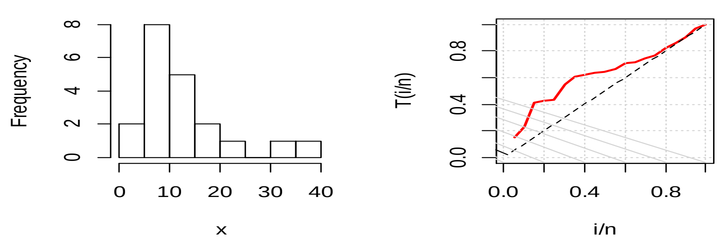

Figure 27. The skewed to right data of 20 items and the values

28- The following skewed to right, a complete set of data, discussed by [17], reports the failure times of 20 electric bulbs and the observations are:

1.32, 12.37, 6.56, 5.05, 11.58, 10.56, 21.82, 3.60, 1.33, 12.62, 5.36, 7.71, 3.53, 19.61, 36.63, 0.39, 21.35, 7.22, 12.42, 8.92.

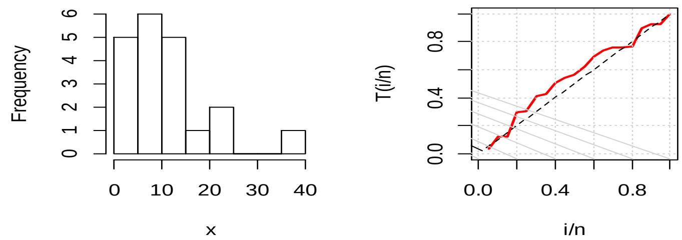

Figure 28. The skewed to the right of the failure times of 20 electric bulbs and observations

29- The following skewed to left, a set of complete data, discussed by [17], and reports the failure times of 20 identical components. The values are:

15.32, 8.29, 8.09, 11.89, 11.03, 10.54, 4.51, 1.79, 7.93, 6.29, 5.46, 2.87, 11.12, 11.23, 3.58, 9.74, 8.45, 2.99, 3.14, 1.80.

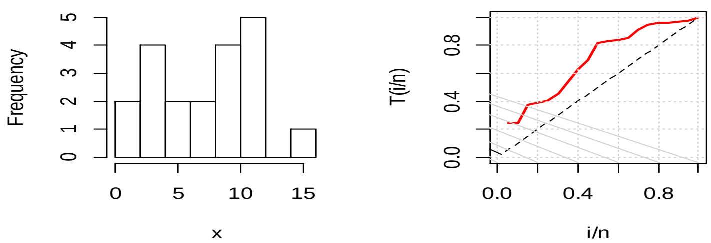

Figure 29. The skewed to left of the failure times of 20 identical components

30- The following bi-modal, a set of complete data discussed by [17], reports the lifetimes of 20 electronic components. The observations are:

0.03, 0.12, 0.22, 0.35, 0.73, 0.79, 1.25, 1.41, 1.52, 1.79, 1.80, 1.94, 2.38, 2.40, 2.87, 2.99, 3.14, 3.17, 4.72, 5.09.

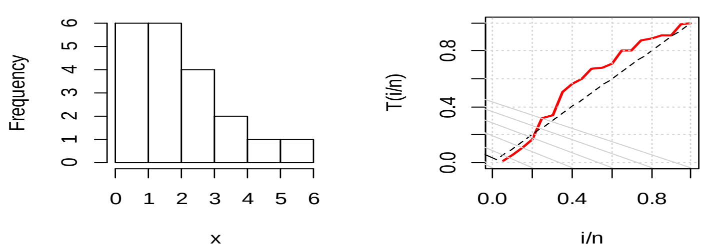

Figure 30. Bi-modal of the lifetimes of 20 electronic components

31- The following set of complete left skewed data, discussed by [17], reports the failure times of 20 components. The values are:

0.481, 1.196, 1.438, 1.797, 1.811, 1.831, 1.885, 2.104, 2.133, 2.144, 2.282, 2.322, 2.334, 2.341, 2.428, 2.447, 2.511, 2.593, 2.715, 3.218.

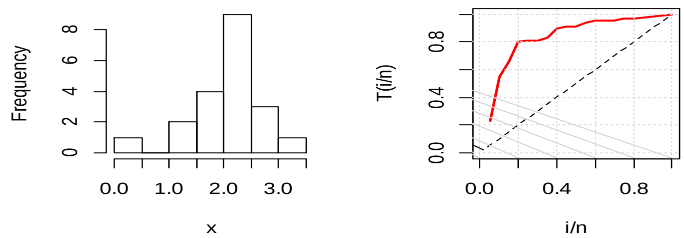

Figure 31. The left-skewed data of the failure times of 20 component

32- The following censored skewed to right data, discussed by [17], contains 50 items, is tested and the test is stopped after the 40-th failure.

0.602, 0.603, 0.603, 0.615, 0.652, 0.663, 0.688, 0.705, 0.761, 0.770, 0.868, 0.884, 0.898, 0.901, 0.911, 0.918, 0.935, 0.953, 0.983, 1.009, 1.040, 1.097, 1.097, 1.148, 1.296, 1.343, 1.422, 1.540, 1.555, 1.653, 1.752, 1.885, 2.015, 2.015, 2.030, 2.040, 2.123, 2.175, 2.443, 2.548.

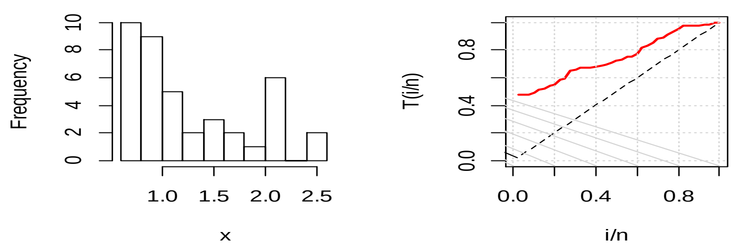

Figure 32. The skewed to right data of 50 items after the 40-th failure

33- A complete set of tri-modal data, discussed by [17], contains 20 components failure times. The observations are:

0.072, 0.477, 1.592, 2.475, 3.597, 4.763, 5.284, 7.709, 7.867, 8.661, 8.663, 9.511, 10.636, 10.729, 11.501, 12.089, 13.036, 13.949, 16.169, 19.809.

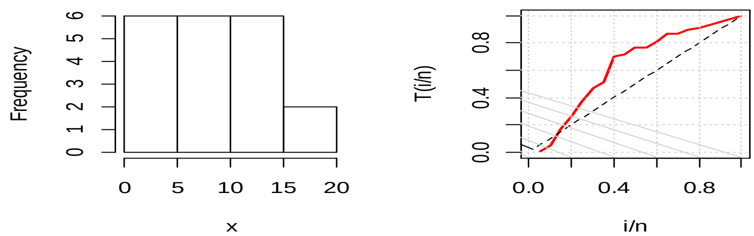

Figure 33. The tri-modal data of 20 components failure times

34- This censored tri-modal data contains 30 items that is tested when test is stopped after 20-th failure. The following data discussed by [17] and the values are:

0.0014, 0.0623, 1.3826, 2.0130, 2.5274, 2.8221, 3.1544, 4.9835, 5.5462, 5.8196, 5.8714, 7.4710, 7.5080, 7.6667, 8.6122, 9.0442, 9.1153, 9.6477, 10.1547, 10.7582.

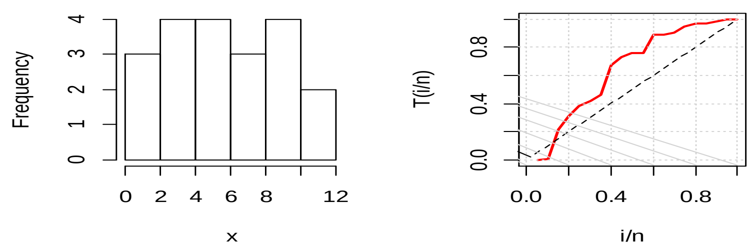

Figure 34. The tri-modal data contains 30 items after 20-th failure

35- A list of complete extreme natured skewed to right data, discussed by [17], represents the failure times of 20 components, and the values are:

2.968, 4.229, 6.560, 6.662, 7.110, 8.608, 8.851, 9.763, 9.773, 10.578, 19.136, 30.112, 37.386, 48.442, 54.145, 57.337, 57.637, 70.175, 79.333, 85.283.

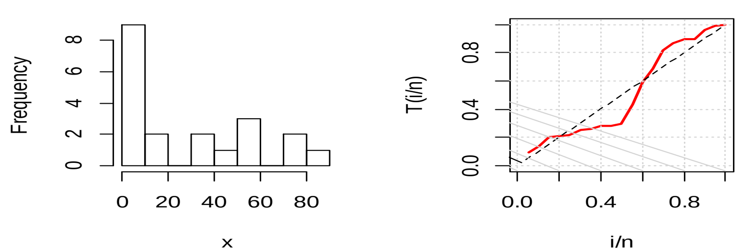

Figure 35. The skewed to right data of the failure times of 20 components

36- A list of complete extreme natured right skewed data, discussed by [17], represents the failure times of 20 components and the observation are:

0.0003, 0.0298, 0.1648, 0.3529, 0.4044, 0.5712, 0.5808, 0.7607, 0.8188, 1.1296, 1.2228, 1.2773, 1.9115, 2.2333, 2.3791, 3.0916, 3.4999, 3.7744, 7.4339, 13.6866.

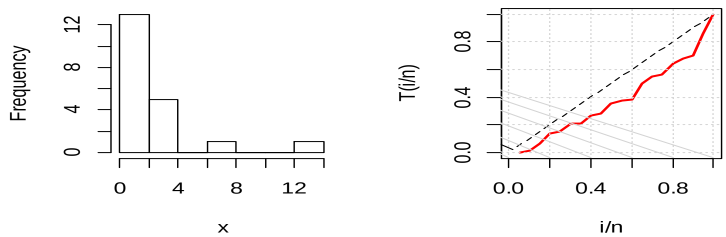

Figure 36. The skewed data of the failure times of 20 components

37- A complete set of extreme natured, skewed to right data discussed by [17], contains the 50 items, put into use at t = 0 (time=t) and failure times (in weeks) are given:

0.013, 0.065, 0.111, 0.111, 0.163, 0.309, 0.426, 0.535, 0.684, 0.747, 0.997, 1.284, 1.304, 1.647, 1.829, 2.336, 2.838, 3.269, 3.977, 3.981, 4.520, 4.789, 4.849, 5.202, 5.291, 5.349, 5.911, 6.018, 6.427, 6.456, 6.572, 7.023, 7.087, 7.291, 7.787, 8.596, 9.388, 10.261, 10.713, 11.658, 13.006, 13.388, 13.842, 17.152, 17.283, 19.418, 23.471, 24.777, 32.795, 48.105.

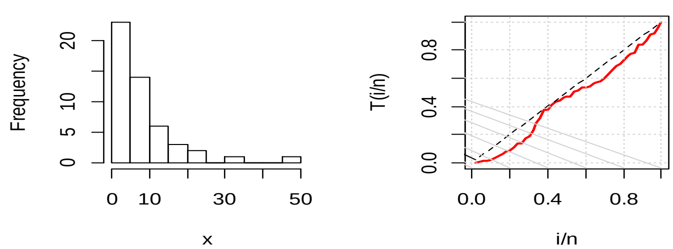

Figure 37. The skewed to right data of the 50 items at t = 0 (time=t) and failure times

38- A complete set of extreme natured, skewed to right data discussed by [17], contains the 50 items, put into use at t = 0 (time=t) and failure times (in weeks) are given:

0.008, 0.017, 0.058, 0.061, 0.084, 0.090, 0.134, 0.238, 0.245, 0.353, 0.374, 0.480, 0.495, 0.535, 0.564, 0.681, 0.686, 0.688, 0.921, 0.959, 1.022, 1.092, 1.260, 1.284, 1.295, 1.373, 1.395, 1.414, 1.760, 1.858, 1.892, 1.921, 1.926, 1.933, 2.135, 2.169, 2.301, 2.320, 2.405, 2.506, 2.598, 2.808, 2.971, 3.087, 3.492, 3.669, 3.926, 4.446, 5.119, 8.596.

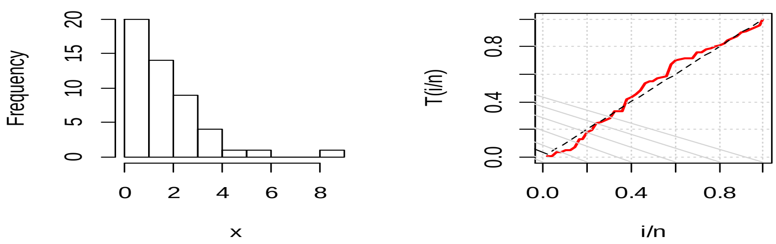

Figure 38. The extreme natured skewed of the 50 items at t = 0 and failure times in weeks

39- A complete set of extreme natured, skewed to right data discussed by [17], explains the failure times of 50 components (Unit: 1000 h), and the observations are:

0.061, 0.073, 0.075, 0.084, 0.086, 0.087, 0.088, 0.089, 0.089, 0.089, 0.099, 0.102, 0.117, 0.118, 0.119, 0.120, 0.123, 0.135, 0.143, 0.168, 0.183, 0.185, 0.191, 0.192, 0.199, 0.203, 0.213, 0.215, 0.257, 0.258, 0.275, 0.297, 0.297, 0.298, 0.299, 0.308, 0.314, 0.315, 0.330, 0.374, 0.388, 0.403, 0.497, 0.714, 0.790, 0.815, 0.817, 0.859, 0.909, 1.286.

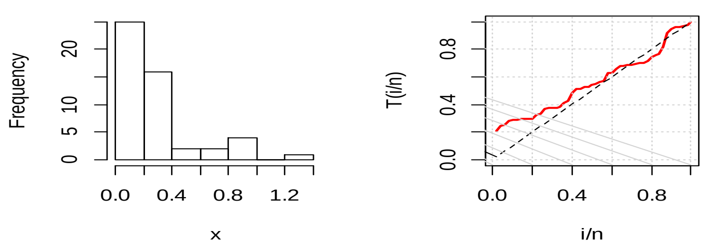

Figure 39. The skewed to right data of the failure times of 50 components

40- A complete set of skewed to right data, discussed by [17] contains the 50 items, put into use at t = 0 (time=t) and failure times are in weeks are given:

1.578, 1.582, 1.858, 2.595, 2.710, 2.899, 2.940, 3.087, 3.669, 3.848, 4.740, 4.848, 5.170, 5.783, 5.866, 5.872, 6.152, 6.406, 6.839, 7.042, 7.187, 7.262, 7.466, 7.479, 7.481, 8.292, 8.443, 8.475, 8.587, 9.053, 9.172, 9.229, 9.352, 10.046, 11.182,11.270, 11.490, 11.623, 11.848, 12.695, 14.369, 14.812, 15.662, 16.296, 16.410, 17.181, 17.675, 19.742, 29.022, 29.047.

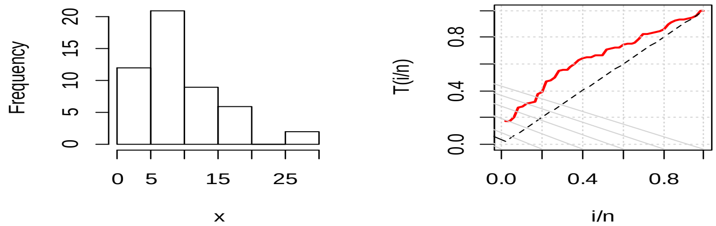

Figure 40. The skewed to right data of the 50 items at t = 0 and failure times in weeks

41- The following set of skewed to right data, discussed by [17], presents a complete list of observations and the values are:

0.032, 0.035, 0.104, 0.169, 0.196, 0.260, 0.326, 0.445, 0.449, 0.496, 0.543, 0.544, 0.577, 0.648, 0.666, 0.742, 0.757, 0.808, 0.857, 0.858, 0.882, 1.005, 1.025, 1.472, 1.916, 2.313, 2.457, 2.530, 2.543, 2.617, 2.835, 2.940, 3.002, 3.158, 3.430, 3.459, 3.502, 3.691, 3.861, 3.952, 4.396, 4.744, 5.346, 5.479, 5.716, 5.825, 5.847, 6.084, 6.127, 7.241, 7.560, 8.901, 9.000, 10.482, 11.133.

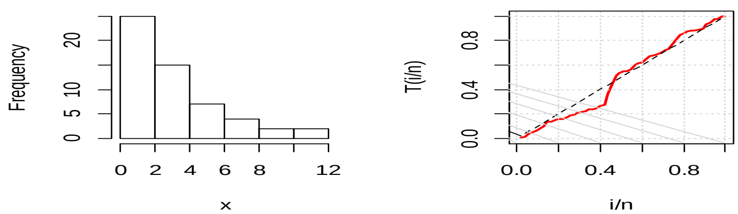

Figure 41. The skewed to right data and observations of the values

42- The following skewed to right figures discussed by [17], are the failure times of eight components at three different temperatures 100, 120, 140. The observations are:

14.712, 32.644, 61.979, 65.521, 105.50, 114.60, 120.40, 138.50, 8.610, 11.741, 54.535, 55.047, 58.928, 63.391, 105.18, 113.02, 2.998, 5.016, 15.628, 23.040, 27.851, 37.843, 38.050, 48.226.

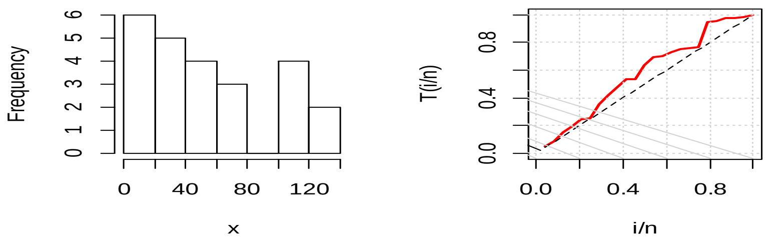

Figure 42. The skewed to right of the failure times of eight components

43- The following skewed to right observations discussed by [17], are the accelerated life testing of 40 items with change in stress from 100 to 150 at time = 15 given by:

0.13, 0.62, 0.75, 0.87, 1.56, 2.28, 3.15, 3.25, 3.55, 4.49, 4.50, 4.61, 4.79, 7.17, 7.31, 7.43, 7.84, 8.49, 8.94, 9.40, 9.61, 9.84, 10.58, 11.18, 11.84, 13.28, 14.47, 14.79, 15.54, 16.90, 17.25, 17.37, 18.69, 18.78, 19.88, 20.06, 20.10, 20.95, 21.72, 23.87.

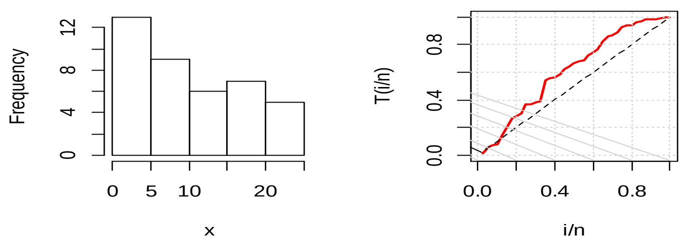

Figure 43. The skewed to right accelerated life testing of 40 items

44- The following bi-modal a set of data, discussed by [17], reports the number of shocks before failure are given:

2, 3, 6, 6, 7, 9, 9, 10, 10, 11, 12, 12, 12, 13, 13, 13, 15, 16, 16, 18.

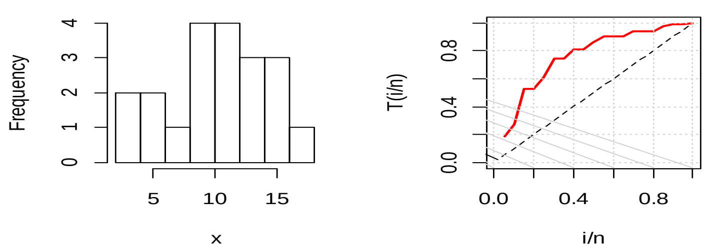

Figure 44. Bi-modal a set of data of the number of shocks before failure

45- The following skewed to right, a set of censored data, discussed by [17], contains the 20 items subjected to shocks and testing stopped after 14 shocks are given:

1, 3, 3, 4, 4, 4, 4, 5, 5, 6, 6, 7, 10, 11, 12, 14.

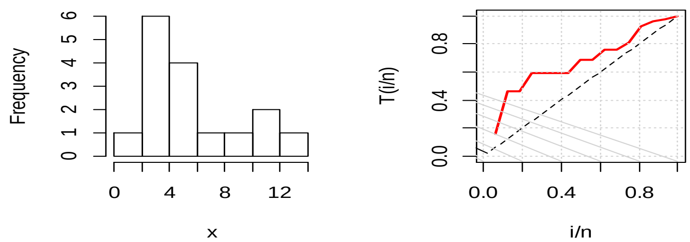

Figure 45. The skewed to right of the 20 items subjected to shocks

46- The following skewed to right, a dataset presents the time between failures for repairable item, discussed by [17]. The observations are:

1.43, 0.11, 0.71, 0.77, 2.63, 1.49, 3.46, 2.46, 0.59, 0.74, 1.23, 0.94, 4.36, 0.40, 1.74, 4.73, 2.23, 0.45, 0.70, 1.06, 1.46, 0.30, 1.82, 2.37, 0.63, 1.23, 1.24, 1.97, 1.86, 1.17.

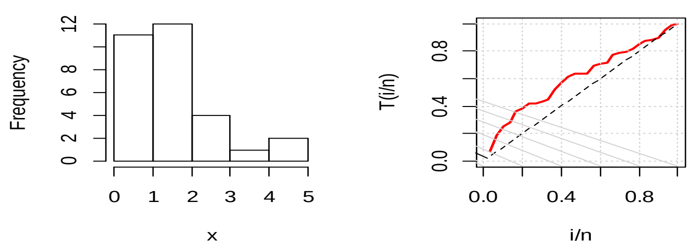

Figure 46. The skewed to the right of the time between failures for repairable item

47- The following bi-modal observations present the time to failure (in hours) for a non-repairable item, discussed by [17] and the observations are:

156.6, 108.0, 289.8, 198.0, 84.1, 51.2, 12.4, 59.1, 35.5, 6.3.

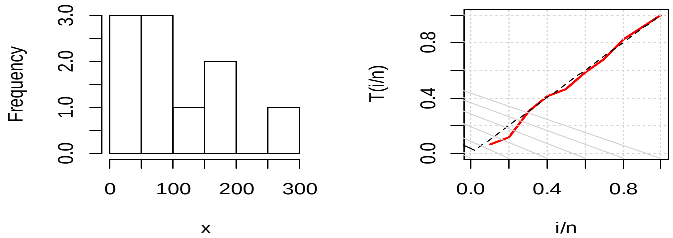

Figure 47. Bi-modal observations present the time to failure (in hours) for a non-repairable item

48- This set of data discussed by [18], hold skewed to the right trend, present the soil fertility influence and the characterization of the biologic fixation of N2 for the Dimorphandra wilsonii frizz growth. The phosphorus concentration, in the leaves, for 128 plants are:

0.22, 0.17, 0.11, 0.10, 0.15, 0.06, 0.05, 0.07, 0.12, 0.09, 0.23, 0.25, 0.23, 0.24, 0.20, 0.08, 0.11, 0.12, 0.10, 0.06, 0.20, 0.17, 0.20, 0.11, 0.16, 0.09, 0.10, 0.12, 0.12, 0.10, 0.09, 0.17, 0.19, 0.21, 0.18, 0.26, 0.19, 0.17, 0.18, 0.20, 0.24, 0.19, 0.21, 0.22, 0.17, 0.08, 0.08, 0.06, 0.09, 0.22, 0.23, 0.22, 0.19, 0.27, 0.16, 0.28, 0.11, 0.10, 0.20, 0.12, 0.15, 0.08, 0.12, 0.09, 0.14, 0.07, 0.09, 0.05, 0.06, 0.11, 0.16, 0.20, 0.25, 0.16, 0.13, 0.11, 0.11, 0.11, 0.08, 0.22, 0.11, 0.13, 0.12, 0.15, 0.12, 0.11, 0.11, 0.15, 0.10, 0.15, 0.17, 0.14, 0.12, 0.18, 0.14, 0.18, 0.13, 0.12, 0.14, 0.09, 0.10, 0.13, 0.09, 0.11, 0.11, 0.14, 0.07, 0.07, 0.19, 0.17, 0.18, 0.16, 0.19, 0.15, 0.07, 0.09, 0.17, 0.10, 0.08, 0.15, 0.21, 0.16, 0.08, 0.10, 0.06, 0.08, 0.12, 0.13.

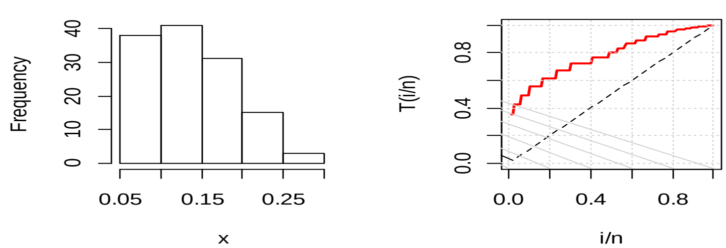

Figure 48. The skewed to right trend, present the soil fertility influence

49- The following skewed to right, 20 items put on test simultaneously and their ordered failure times discussed by [19]. The ordered observed data is as follow:

0.0009, 0.004, 0.0142, 0.0221, 0.0261, 0.0418, 0.0473, 0.0834, 0.1091, 0.1252, 0.1404, 0.1498, 0.175, 0.2031, 0.2099, 0.2168, 0.2918, 0.3465, 0.4035, 0.6143.

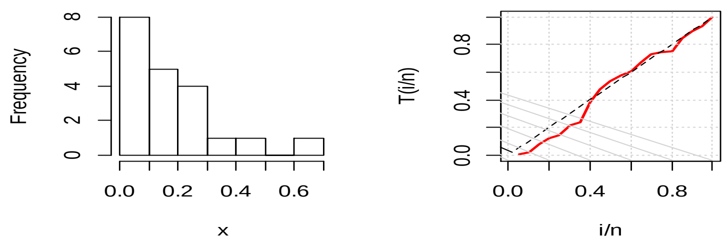

Figure 49. The right skewed of 20 items put on test simultaneously and their ordered failure times

50- The following dataset which is skewed to right, reported by [20], present the SAR image modeling on oil slick visibility in ocean. The observations are:

0.01149687, 0.01250427, 0.01528162, 0.01570864, 0.01802599, 0.01894287, 0.01911615, 0.01935418, 0.01992964, 0.02017052, 0.02051137, 0.02082554, 0.02185369, 0.02260664, 0.02293175, 0.02296903, 0.02317232, 0.02338895, 0.02358412, 0.02363688, 0.02396332, 0.02407404, 0.02585229, 0.02647153, 0.02665159, 0.02667463, 0.02721631, 0.02775543, 0.02777823, 0.02784315, 0.02792585, 0.02833025, 0.02839673, 0.02856023, 0.02861129, 0.02892729, 0.02931118, 0.02941171, 0.02942552, 0.03024757, 0.03101604, 0.03141554, 0.03224484, 0.03228633, 0.03232158, 0.03384829, 0.03402714, 0.03424702, 0.03427167, 0.03445653, 0.03453897, 0.03474018, 0.03501506, 0.03578667, 0.03598676, 0.03752478, 0.03754972, 0.03763689, 0.03803634, 0.0382402, 0.03879451, 0.03893850, 0.03989288, 0.04063699, 0.04111884, 0.04164984, 0.0416827, 0.04230256, 0.0427892, 0.04341392, 0.04367883, 0.04526951, 0.04538165, 0.0458550, 0.0462939, 0.04638059, 0.04639203, 0.04647379, 0.04675854, 0.04694617, 0.04768521, 0.04783208, 0.0483232, 0.04891223, 0.04971199, 0.05092829, 0.05177016, 0.05190274, 0.05229843, 0.05260086, 0.05274564, 0.05385335, 0.0539581, 0.0544991, 0.05508701, 0.05515739, 0.05547253, 0.05562469, 0.05611064, 0.05686707, 0.05705985, 0.05840242, 0.05941767, 0.05983544, 0.0608492, 0.06187658, 0.06204657, 0.06370583, 0.06403044, 0.06442861, 0.06560329, 0.0661218, 0.06653712, 0.06816631, 0.07138552, 0.07589816, 0.07643031, 0.0774606, 0.07915612, 0.08028217, 0.08059592, 0.0847016, 0.08566783, 0.09340851, 0.09429808, 0.09665179, 0.1003492, 0.1060528, 0.1092498, 0.1206784, 0.1257918.

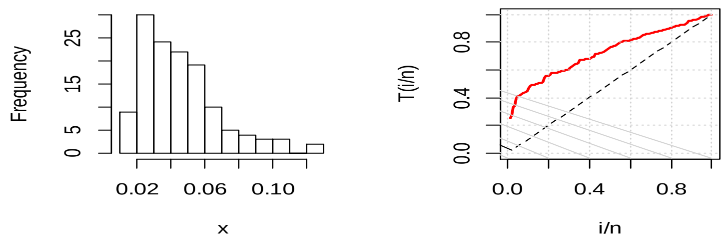

Figure 50. The skewed to right, from the SAR image modeling on oil slick visibility in ocean

51- The following right skewed dataset presented by [21] is obtained from the measurements on petroleum rock samples. The data consists of 48 rock samples from a petroleum reservoir. The dataset corresponds to twelve core samples from petroleum reservoirs that were sampled by four cross-sections. Each core sample was measured for permeability and each cross-section has the following variables: the total area of pores, the total perimeter of pores and shape. We analyze the shape perimeter by squared (area) variable and the observations are:

0.0903296, 0.2036540, 0.2043140, 0.2808870, 0.1976530, 0.3286410, 0.1486220, 0.1623940, 0.2627270, 0.1794550, 0.3266350, 0.2300810, 0.1833120, 0.1509440, 0.2000710, 0.1918020, 0.1541920, 0.4641250, 0.1170630, 0.1481410, 0.1448100, 0.1330830, 0.2760160, 0.4204770, 0.1224170, 0.2285950, 0.1138520, 0.2252140, 0.1769690, 0.2007440, 0.1670450, 0.2316230, 0.2910290, 0.3412730, 0.4387120, 0.2626510, 0.1896510, 0.1725670, 0.2400770, 0.3116460, 0.1635860, 0.1824530, 0.1641270, 0.1534810, 0.1618650, 0.2760160, 0.2538320, 0.2004470.

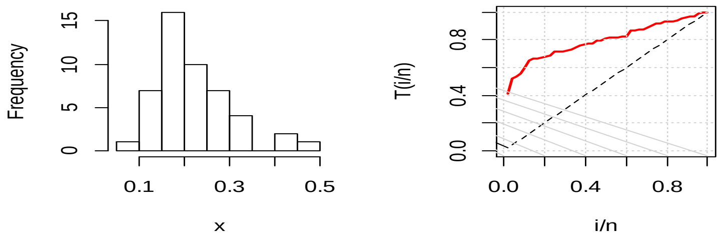

Figure 51. The right skewed from the measurements on 48 petroleum rock samples

52-The symmetric behavior of the following dataset, discussed by [22], consists of 50 observations relates to holes operation on jobs made of iron sheet. This dataset is as follows:

0.04, 0.02, 0.06, 0.12, 0.14, 0.08, 0.22, 0.12, 0.08, 0.26, 0.24, 0.04, 0.14, 0.16, 0.08, 0.26, 0.32, 0.28, 0.14, 0.16, 0.24, 0.22, 0.12, 0.18, 0.24, 0.32, 0.16, 0.14, 0.08, 0.16, 0.24, 0.16, 0.32, 0.18, 0.24, 0.22, 0.16, 0.12, 0.24, 0.06, 0.02, 0.18, 0.22, 0.14, 0.06, 0.04, 0.14, 0.26, 0.18, 0.16.

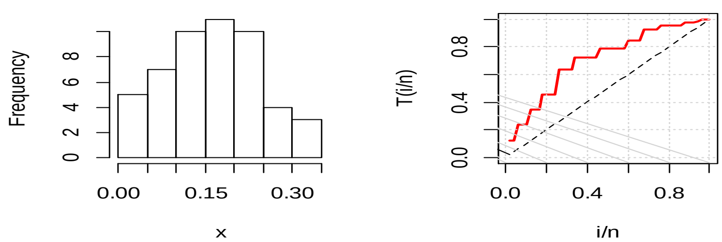

Figure 52. The symmetric behavior of 50 observations of holes operation

53- The following skewed to right data, discussed by [23], and is the comparison of the two different algorithms called SC16 and P3 for estimating unit capacity factors. The values resulted from the algorithm SC16 are:

0.853, 0.759, 0.866, 0.809, 0.717, 0.544, 0.492, 0.403, 0.344, 0.213, 0.116, 0.116, 0.092, 0.070, 0.059, 0.048, 0.036, 0.029, 0.021, 0.014, 0.011, 0.008, 0.006.

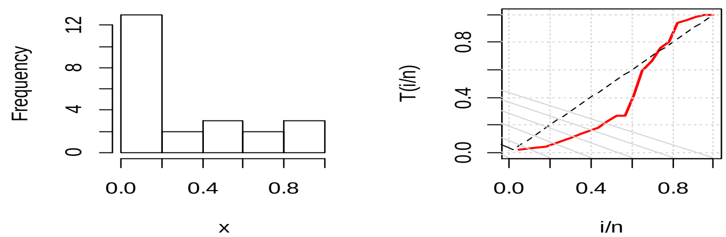

Figure 53. The right skewed of comparison of the two different algorithms called SC16 and P3

54- The following moderately skewed to right dataset, discussed by [24], explains the fatigue fracture of Kevlar 373/epoxy subjected to constant pressure at 90 % stress level until all had failed. The observations are:

0.0251, 0.0886, 0.0891, 0.2501, 0.3113, 0.3451, 0.4763, 0.5650, 0.5671, 0.6566, 0.6748, 0.6751, 0.6753, 0.7696, 0.8375, 0.8391, 0.8425, 0.8645, 0.8851, 0.9113, 0.9120, 0.9836, 1.0483, 1.0596, 1.0773, 1.1733, 1.2570, 1.2766, 1.2985, 1.3211, 1.3503, 1.3551, 1.4595, 1.4880, 1.5728, 1.5733, 1.7083, 1.7263, 1.7460, 1.7630, 1.7746, 1.8275, 1.8375, 1.8503, 1.8808, 1.8878, 1.8881, 1.9316, 1.9558, 2.0048, 2.0408, 2.0903, 2.1093, 2.1330, 2.2100, 2.2460, 2.2878, 2.3203, 2.3470, 2.3513, 2.4951, 2.5260, 2.9911, 3.0256, 3.2678, 3.4045, 3.4846, 3.7433, 3.7455, 3.9143, 4.8073, 5.4005, 5.4435, 5.5295, 6.5541, 9.0960.

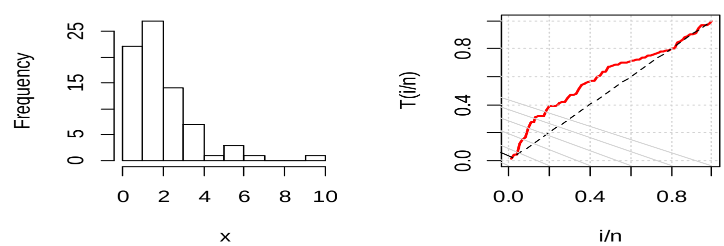

Figure 54. The moderately skewed to right for fatigue fracture of Kevlar 373/epoxy subjected to constant pressure at 90 % stress level until all had failed

55- The following symmetric trend of the dataset, discussed by [25], presents the fracture toughness of material Alumina (AI2O3) and the values are:

5.5, 5, 4.9, 6.4, 5.1, 5.2, 5.2,5, 4.7, 4, 4.5, 4.2, 4.1, 4.56, 5.01, 4.7, 3.13, 3.12, 2.68, 2.77, 2.7, 2.36, 4.38, 5.73, 4.35, 6.81, 1.91, 2.66, 2.61, 1.68, 2.04, 2.08, 2.13, 3.8, 3.73, 3.71, 3.28, 3.9, 4, 3.8, 4.1, 3.9, 4.05, 4, 3.95, 4, 4.5, 4.5, 4.2, 4.55, 4.65, 4.1, 4.25, 4.3, 4.5, 4.7, 5.15, 4.3, 4.5, 4.9, 5, 5.35, 5.15, 5.25, 5.8, 5.85, 5.9, 5.75, 6.25, 6.05, 5.9, 3.6, 4.1, 4.5, 5.3, 4.85, 5.3, 5.45, 5.1, 5.3, 5.2, 5.3, 5.25, 4.75, 4.5, 4.2, 4, 4.15, 4.25, 4.3, 3.75, 3.95, 3.51, 4.13, 5.4, 5, 2.1, 4.6, 3.2, 2.5, 4.1, 3.5, 3.2, 3.3, 4.6, 4.3, 4.3, 4.5, 5.5, 4.6, 4.9, 4.3, 3, 3.4, 3.7, 4.4, 4.9, 4.9, 5.

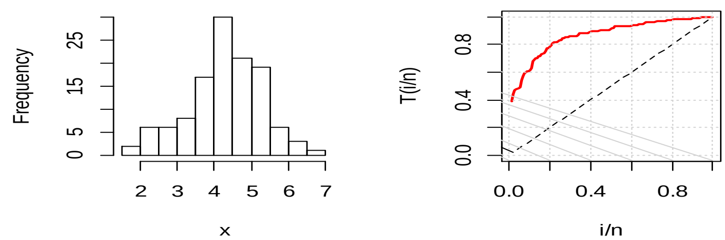

Figure 55. The symmetric for fracture toughness of material Alumina (AI2O3)

56- The following bi-modal dataset, discussed by [26], is obtained from the banking sector, discusses the waiting time (in minutes) before the customer received service in a bank. The values are:

0.8, 0.8, 1.3, 1.5, 1.8, 1.9, 1.9, 2.1, 2.6, 2.7, 2.9, 3.1, 3.2, 3.3, 3.5, 3.6, 4.0, 4.1, 4.2, 4.2, 4.3, 4.3, 4.4, 4.4, 4.6, 4.7, 4.7, 4.8, 4.9, 4.9, 5.0, 5.3, 5.5, 5.7, 5.7, 6.1, 6.2, 6.2, 6.2, 6.3, 6.7, 6.9, 7.1, 7.1, 7.1, 7.1, 7.4, 7.6, 7.7, 8.0, 8.2, 8.6, 8.6, 8.6, 8.8, 8.8, 8.9, 8.9, 9.5, 9.6, 9.7, 9.8, 10.7, 10.9, 11.0, 11.0, 11.1 ,11.2, 11.2, 11.5,11.9, 12.4, 12.5, 12.9, 13.0, 13.1, 13.3, 13.6, 13.7, 13.9,14.1, 15.4, 15.4, 17.3, 17.3, 18.1, 18.2, 18.4, 18.9, 19.0, 19.9, 20.6, 21.3, 21.4, 21.9, 23.0, 27.0, 31.6, 33.1, 38.5.

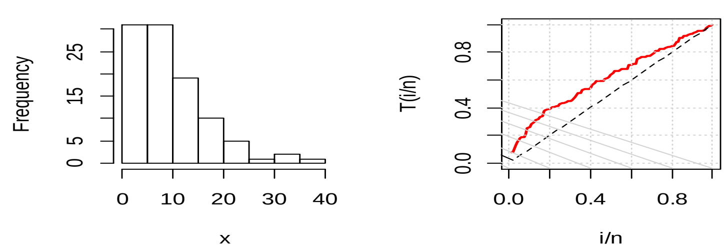

Figure 56. The bi-modal for banking sector, discusses the waiting time (in minutes) before the customer received service in a bank

57- The following symmetric observations discussed by [27], are the strength measured in GPA for single carbon fibers and impregnated 1000-carbon fiber tows. Single fibers were tested under tension at gauge length of 10mm. It is given by:

1.901, 2.132, 2.203, 2.228, 2.257, 2.350, 2.361, 2.396, 2.397, 2.445, 2.454, 2.474, 2.518, 2.522, 2.525, 2.532, 2.575, 2.614, 2.616, 2.618, 2.624, 2.659, 2.675, 2.738, 2.740, 2.856, 2.917, 2.928, 2.937, 2.937, 2.977, 2.996, 3.030, 3.125, 3.139, 3.145, 3.220, 3.223, 3.235, 3.243, 3.264, 3.272, 3.294, 3.332, 3.346, 3.377, 3.408, 3.435, 3.493, 3.501, 3.537, 3.554, 3.562, 3.628, 3.852, 3.871, 3.886, 3.971, 4.024, 4.027, 4.225, 4.395, 5.020.

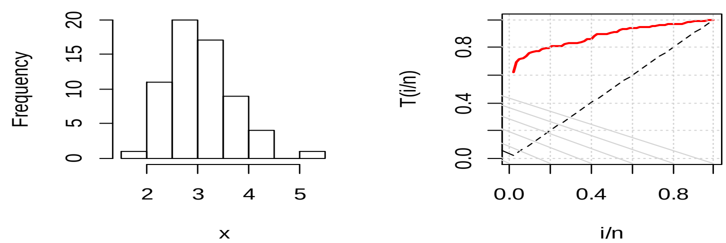

Figure 57. The symmetric for strength measured in GPA for single carbon fibers and impregnated 1000-carbon fiber tows

58- The following extreme set of observations skewed to right, introduced by [28], present the patients suffering (survival time) from acute Myelogenous Leukemia and it is given:

65, 156, 100, 134, 16, 108, 121, 4, 39, 143, 56, 26, 22, 1, 1, 5, 65, 56, 65, 17, 7, 16, 22, 3, 4, 2, 3, 8, 4, 3, 30, 4, 43.

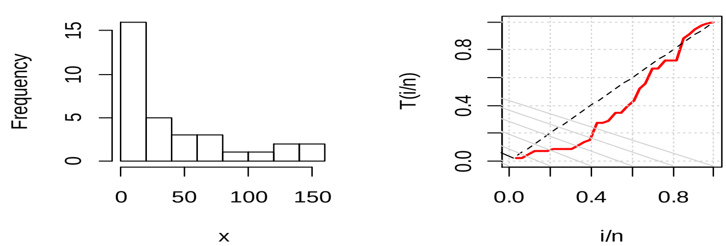

Figure 58. The right skewed for the patients suffering (survival time) from acute Myelogenous Leukemia

59- The following extreme skewed to right data, is achieved from annual flood discharge rates of the Floyd River, discussed by [29], the observations are:

1460, 4050, 3570, 2060, 1300, 1390, 1720, 6280, 1360, 7440, 5320, 1400, 3240, 2710, 4520, 4840, 8320, 13900, 71500, 6250, 2260, 318, 1330, 970, 1920, 15100, 2870, 20600, 3810, 726, 7500, 7170, 2000, 829, 17300, 4740, 13400, 2940, 5660.

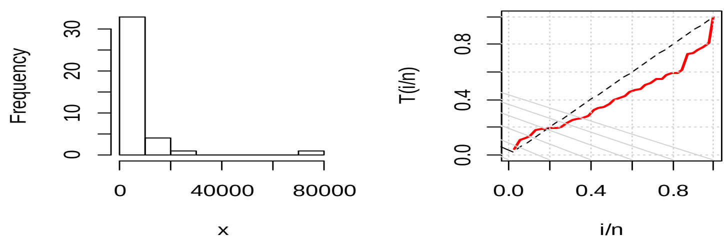

Figure 59. The extreme nature for annual flood discharge rates of the Floyd River

60- The following set of data, introduced by [30], presents the moderately skewed to left trend of the gauge lengths of 20 mm, and the observations are:

1.312, 1.314, 1.479, 1.552, 1.700, 1.803, 1.861, 1.865, 1.944, 1.958, 1.966, 1.997, 2.006, 2.021, 2.027, 2.055, 2.063, 2.098, 2.140, 2.179, 2.224, 2.240, 2.253, 2.270, 2.272, 2.274, 2.301, 2.301, 2.359, 2.382, 2.382, 2.426, 2.434, 2.435, 2.478, 2.490, 2.511, 2.514, 2.535, 2.554, 2.566, 2.570, 2.586, 2.629, 2.633, 2.642, 2.648, 2.684, 2.697, 2.726, 2.770, 2.773, 2.800, 2.809, 2.818, 2.821, 2.848, 2.880, 2.809, 2.818, 2.821, 2.848, 2.880, 2.954, 3.012, 3.067, 3.084, 3.090, 3.096, 3.128, 3.233, 3.433, 3.585, 3.585.

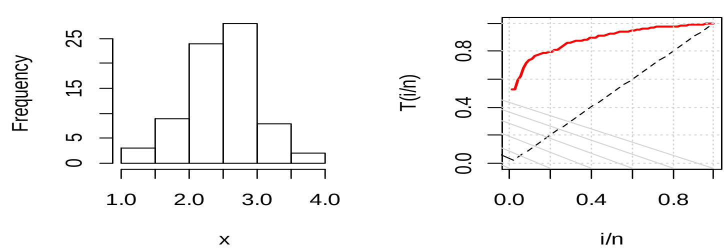

Figure 60. The moderately skewed to left trend of the gauge lengths of 20 mm

61- The following set of data discussed by [31], indicates the skewed to right trend, gives the number of cycles to failure for 25 100-cm specimens of yarn, is tested at a particular strain level and they are:

15, 20, 38, 42, 61, 76, 86, 98, 121, 146, 149, 157, 175, 176, 180, 180, 198, 220, 224, 251, 264, 282, 321, 325, 653.

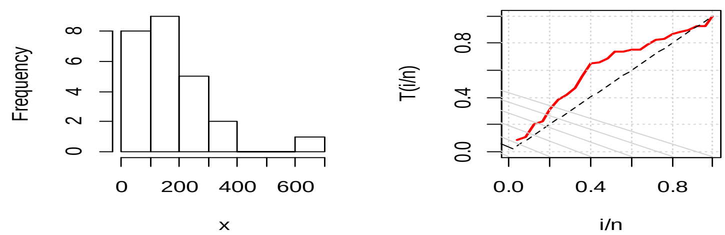

Figure 61. The skewed to right trend of the number of cycles to failure for 25 100-cm specimens of yarn

62- The following real time extreme natured a set of bathtub shaped failure rate data, reported by [32], presents the times of 30 electronic components taken from power-line voltage spikes during electric storms. The values are:

275, 13, 147, 23, 181, 30, 65, 10, 300, 173, 106, 300, 300, 212, 300, 300, 300, 2, 261, 293, 88,247, 28, 143, 300, 23, 300, 80, 245, 266.

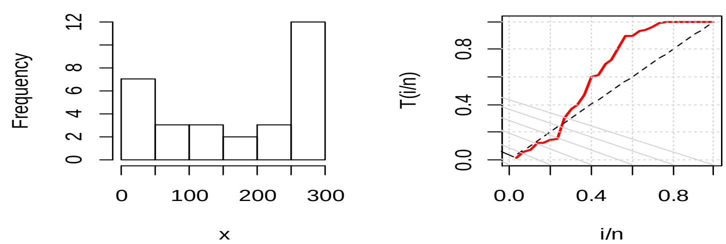

Figure 62. The real time extreme natured of bathtub shaped failure rate data

63- The following skewed to left data presents the lifetime of a certain device reported by [33], and the observations are:

0.0094, 0.05, 0.4064, 4.6307, 5.1741, 5.8808, 6.3348, 7.1645, 7.2316, 8.2604, 9.2662, 9.3812, 9.5223, 9.8783, 9.9346, 10.0192, 10.4077, 10.4791, 11.076, 11.325, 11.5284, 11.9226, 12.0294, 12.074, 12.1835, 12.3549, 12.5381, 12.8049, 13.4615, 13.853.

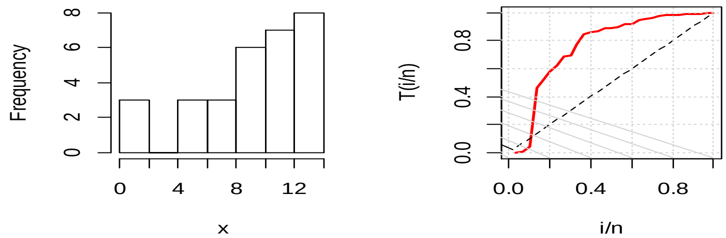

Figure 63. The skewed to the left of the lifetime of a certain device

64- The following skewed to right an extreme natured set of data, deals with the time to failure of 18 electronic devices discussed by [34], and the observations are:

5, 11, 21, 31, 46, 75, 98, 122, 145, 165, 195, 224,245, 293, 321, 330, 350, 420.

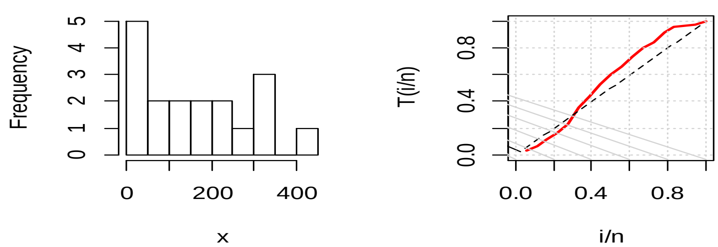

Figure 64. The skewed to right with the time to failure of 18 electronic devices

65- The following skewed to left life time data developed by [35], represents the time to failure (103h) of turbocharger of one type of engine. The values are:

1.6, 2.0, 2.6, 3.0, 3.5, 3.9, 4.5, 4.6, 4.8, 5.0, 5.1, 5.3, 5.4, 5.6, 5.8, 6.0, 6.0, 6.1, 6.3, 6.5, 6.5, 6.7, 7.0, 7.1, 7.3, 7.3, 7.3, 7.7, 7.7, 7.8, 7.9, 8.0, 8.1, 8.3, 8.4, 8.4, 8.5, 8.7, 8.8, 9.0.

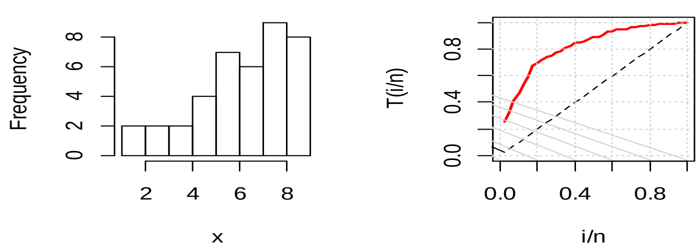

Figure 65. The skewed to left life of the time to failure of turbocharger of one type of engine

66- The following moderately skewed to right a set of data presented by [36], deals in the failure time of 84 windshields for a particular model of aircraft (the unit for measurement is 1000 hours). The values are:

0.040, 1.866, 2.385, 3.443, 0.301, 1.876, 2.481, 3.467, 0.309, 1.899, 2.610, 3.478, 0.557, 1.911, 2.625, 3.578, 0.943, 1.912, 2.632, 3.595, 1.070, 1.914, 2.646, 3.699, 1.124, 1.981, 2.661, 3.779, 1.248, 2.010, 2.688, 3.924, 1.281, 2.038, 2.82,3, 4.035, 1.281, 2.085, 2.890, 4.121, 1.303, 2.089, 2.902, 4.167, 1.432, 2.097, 2.934, 4.240, 1.480, 2.135, 2.962, 4.255, 1.505, 2.154, 2.964, 4.278, 1.506, 2.190, 3.000, 4.305, 1.568, 2.194, 3.103, 4.376, 1.615, 2.223, 3.114, 4.449, 1.619, 2.224, 3.117, 4.485, 1.652, 2.229, 3.166, 4.570, 1.652, 2.300, 3.344, 4.602, 1.757, 2.324, 3.376, 4.663.

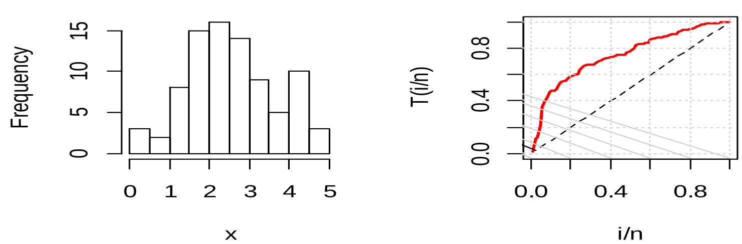

Figure 66. The moderately skewed to right of the failure time of 84 windshields for a particular model of aircraft

67- The following moderately skewed to right a set of data, presented by [36], relates to the service times of 63 Aircraft Windshield (the unit for measurement is 1000 hours). The values are:

0.046, 1.436, 2.592, 0.140, 1.492, 2.600, 0.150, 1.580, 2.670, 0.248, 1.719, 2.717, 0.280, 1.794, 2.819, 0.313, 1.915, 2.820, 0.389, 1.920, 2.878, 0.487, 1.963, 2.950, 0.622, 1.978, 3.003, 0.900, 2.053, 3.102, 0.952, 2.065, 3.304, 0.996, 2.117, 3.483, 1.003, 2.137, 3.500, 1.010, 2.141, 3.622, 1.085, 2.163, 3.665, 1.092, 2.183, 3.695, 1.152, 2.240, 4.015, 1.183, 2.341, 4.628, 1.244, 2.435, 4.806, 1.249, 2.464, 4.881, 1.262, 2.543, 5.140.

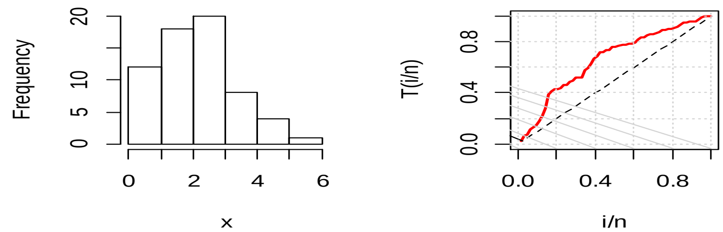

Figure 67. The moderately skewed to the right of the service times of 63 Aircraft Windshield

68- The following set of data reported by [37], exhibit the skewed to right trend and it consists of the waiting times between 65 consecutive eruptions of the Kiama Blowhole. The Kiama Blowhole is a tourist attraction located nearly 120km to the south of Sydney. The swelling of the ocean pushes the water through a hole below a cliff. The water then erupts through an exit usually drenching whoever is nearby. The times between eruptions of 1340 hours starting from July 12th of 1998 were recorded using a digital watch. These data were reported by professor Jim Irish and values are:

83, 51, 87, 60, 28, 95, 8, 27, 15, 10, 18, 16, 29, 54,91, 8, 17, 55, 10, 35,47, 77, 36, 17, 21, 36, 18, 40, 10, 7, 34, 27, 28, 56, 8, 25, 68, 146, 89, 18, 73, 69, 9, 37, 10, 82, 29, 8, 60, 61, 61, 18, 169, 25, 8, 26, 11, 83, 11, 42, 17, 14, 9, 12.

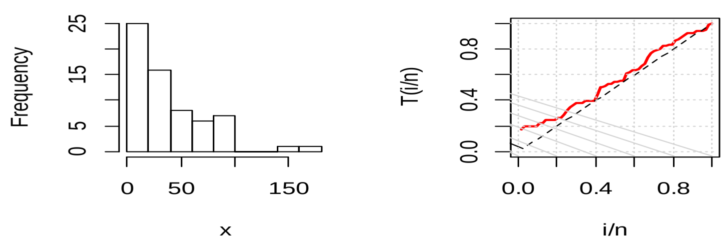

Figure 68. The exhibit the skewed of the waiting times between 65 consecutive eruptions of the Kiama Blowhole

69- The following uncensored extreme natured (skewed to right) a set of data, discussed by [38], corresponding to intervals in days between 109 successive coal-mining disasters in Great Britain, for the period 1875-1951. The values are:

1, 4, 4, 7, 11, 13, 15, 15, 17, 18, 19, 19, 20, 20, 22, 23, 28, 29, 31, 32, 36, 37, 47, 48, 49, 50, 54, 54, 55, 59, 59, 61, 61, 66, 72, 72, 75, 78, 78, 81, 93, 96, 99, 108, 113, 114, 120, 120, 120, 123, 124, 129, 131, 137, 145, 151, 156, 171, 176, 182, 188, 189, 195, 203, 208, 215, 217, 217, 217, 224, 228, 233, 255, 271, 275, 275, 275, 286, 291, 312, 312, 312, 315, 326, 326, 329, 330,336, 338, 345, 348, 354, 361, 364, 369, 378, 390, 457, 467, 498, 517, 566, 644, 745, 871, 1312, 1357, 1613, 1630.

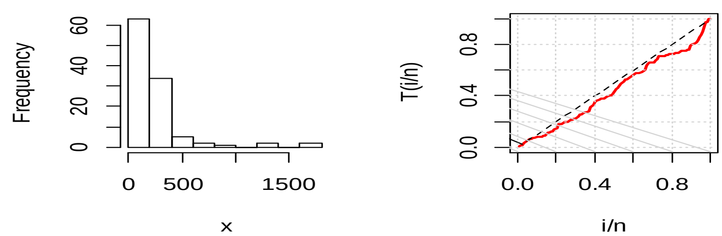

Figure 69. The uncensored extreme natured of intervals in days between 109 successive coal-mining disasters

70- The following skewed to right a set of data, reported [39], presents the failure times of the air conditioning system of an air plane. The values are:

23, 261, 87, 7, 120, 14, 62, 47, 225, 71, 246, 21, 42, 20, 5, 12, 120, 11, 3, 14, 71, 11, 14, 11, 16, 90, 1, 16, 52, 95.

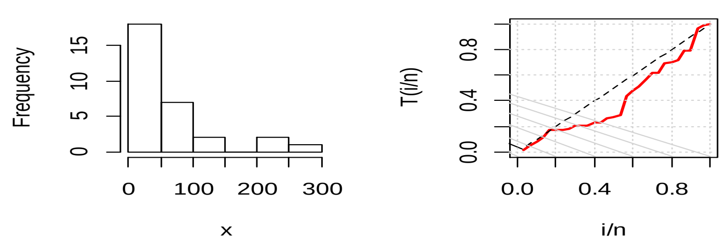

Figure 70. The skewed to right of the failure times of the air conditioning system of an air plane

71- The following skewed to right a set of data, discussed by [40], represents the monthly actual taxes revenue (in 1000 million Egyptian pounds) in Egypt between January 2006 and November 2010. The values are:

5.9, 20.4, 14.9, 16.2, 17.2, 7.8, 6.1, 9.2, 10.2, 9.6, 13.3, 8.5, 21.6, 18.5, 5.1, 6.7, 17, 8.6, 9.7, 39.2, 35.7, 15.7, 9.7, 10, 4.1, 36, 8.5, 8, 9.2, 26.2, 21.9, 16.7, 21.3, 35.4, 14.3, 8.5, 10.6, 19.1, 20.5, 7.1, 7.7, 18.1, 16.5, 11.9, 7, 8.6, 12.5, 10.3, 11.2, 6.1, 8.4, 11, 11.6, 11.9, 5.2, 6.8, 8.9, 7.1, 10.8.

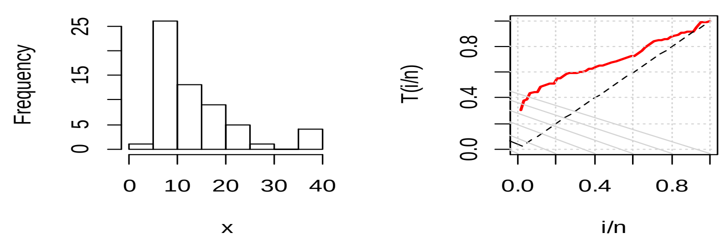

Figure 71. The skewed to right of the monthly actual taxes revenue in Egypt

72- The following skewed to right a set of data, developed by [41], presents the March precipitation (in inches) observations. The values are:

0.77, 1.74, 0.81, 1.2, 1.95, 1.2, 0.47, 1.43, 3.37, 2.2, 3, 3.09, 1.51, 2.1, 0.52, 1.62, 1.31, 0.32, 0.59, 0.81, 2.81, 1.87, 1.18, 1.35, 4.75, 2.48, 0.96, 1.89, 0.9, 2.05.

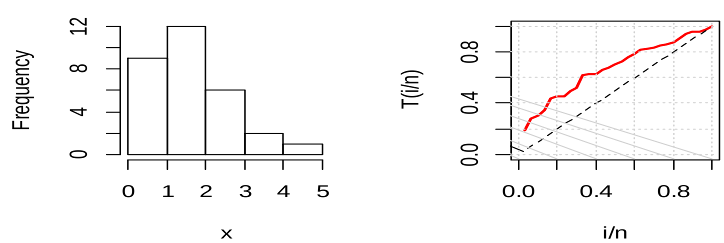

Figure 72. The skewed to right of the March precipitation

73- The following set of a data presents the skewed to right behavior, covered by [42], the repair times (Hours) for an airborne communication transceiver. The values are:

0.50, 0.60, 0.60, 0.70, 0.70, 0.70, 0.80, 0.80, 1.00, 1.00, 1.00, 1.00, 1.10, 1.30, 1.50, 1.50, 1.50, 1.50, 2.00, 2.00, 2.20, 2.50, 2.70, 3.00, 3.00, 3.30, 4.00, 4.00, 4.50, 4.70, 5.00, 5.40, 5.40, 7.00, 7.50, 8.80, 9.00, 10.20, 22.00, 24.50.

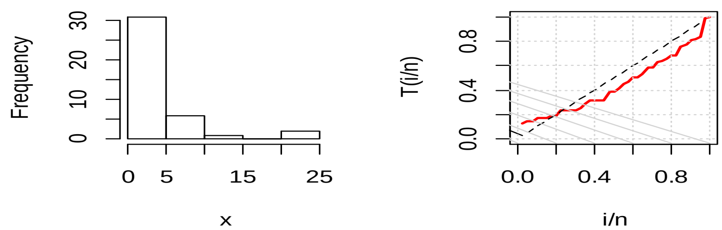

Figure 73. The skewed to right behavior of the repair times for an airborne communication transceiver

74- The following skewed to right a set of data, discussed by [43], presents the total annual rainfall (in inches) during the month of January from 1880 to 1916 recorded at Los Angeles Civic Center. The values are:

1.33, 1.43, 1.01, 1.62, 3.15, 1.05, 7.72, 0.2, 6.03, 0.25, 7.83, 0.25, 0.88, 6.29, 0.94, 5.84, 3.23, 3.7, 1.26, 2.64, 1.17, 2.49, 1.62, 2.1, 0.14, 2.57, 3.85, 7.02, 5.04, 7.27, 1.53, 6.7, 0.07, 2.01, 10.35, 5.42, 13.3.

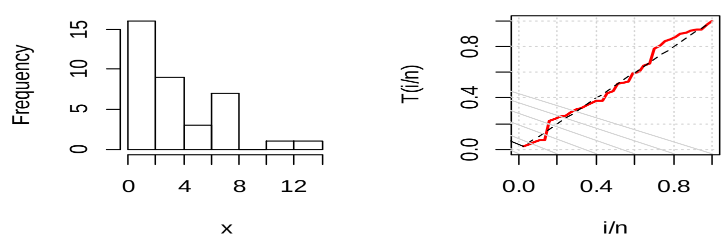

Figure 74. The skewed to the right of the total annual rainfall at Los Angeles Civic Center

75- The following skewed to right a set of data presented by [44], discusses the prices of wooden toys of 31 children in April 1991 at Suffolk craft shop. The values are:

4.2, 1.12, 1.39, 2, 3.99, 2.15, 1.74, 5.81, 1.7, 0.5, 0.99, 11.5, 5.12, 0.9, 1.99, 6.24, 2.6, 3, 12.2, 7.36, 4.75, 11.59, 8.69, 9.8, 1.85, 1.99, 1.35, 10, 0.65, 1.45.

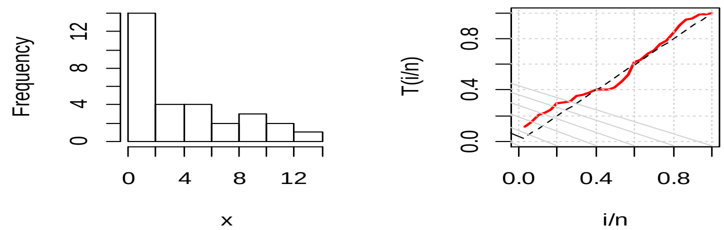

Figure 75. The skewed to right of the prices of wooden toys at Suffolk craft shop

76- This set of data gives the time-to-failure (10^3 h) of turbocharger of one type of engine. This dataset has extreme nature (right skewed) and discussed by [35]. The observation are:

1.6, 2.0, 2.6, 3.0, 3.5, 3.9, 4.5, 4.6, 4.8, 5.0, 5.1, 5.3, 5.4, 5.6, 5.8, 6.0, 6.0, 6.1, 6.3, 6.5, 6.5, 6.7, 7.0, 7.1, 7.3, 7.3, 7.3, 7.7, 7.7, 7.8, 7.9, 80, 8.1, 8.3, 8.4, 8.4, 8.5, 8.7, 8.8, 9.0.

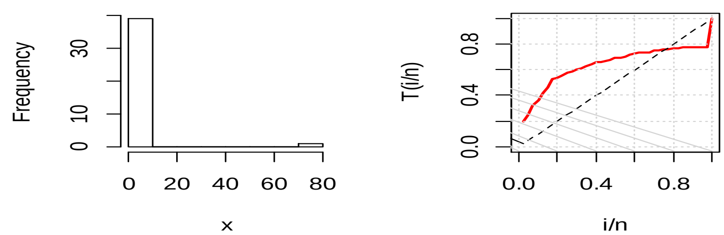

Figure 76. The time-to-failure of turbocharger of one type of engine

77- The following right to skewed data set discussed by [45], is used to correspond the time-to-failure of a polyester/viscose yarn in a textile experiment for testing the tensile fatigue characteristics of yarn. It consists of a sample of 100 cm yarn at 2.3% strain level. The values are:

86, 146, 251, 653, 98, 249, 400, 292, 131, 169, 175, 176, 76, 264, 15, 364, 195, 262, 88, 264, 157, 220, 42, 321, 180, 198, 38, 20, 61, 121, 282, 224, 149, 180, 325, 250, 196, 90, 229, 166, 38, 337, 65, 151, 341, 40, 40, 135, 597, 246, 211, 180, 93, 315, 353, 571, 124, 279, 81, 186, 497, 182, 423, 185, 229, 400, 338, 290, 398, 71, 246, 185, 188, 568, 55, 55, 61, 244, 20, 284, 393, 396, 203, 829, 239, 236, 286, 194, 277, 143, 198, 264, 105, 203, 124, 137, 135, 350, 193, 188.

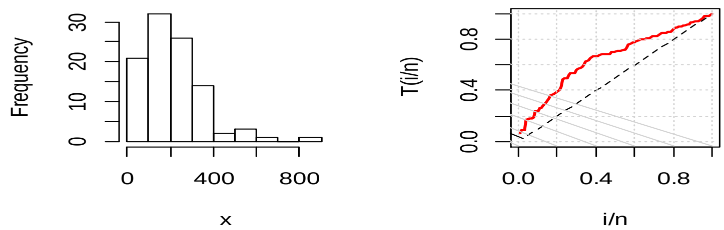

Figure 77. The skewed of the time-to-failure of a polyester/viscose yarn in a textile experiment

78- The following data set consists of the IQ for 52 non-white males, hired by a large insurance company in 1971. This dataset has extreme nature (right skewed), discussed by [46]. The values are:

91, 102, 100, 117, 122, 115, 97, 109, 108, 104, 108, 118, 103, 123, 123, 103, 106,102, 118, 100, 103, 107, 108, 107, 97, 95, 119, 102, 108, 103, 102, 112, 99, 116, 114, 102, 111, 104, 122, 103, 111, 101, 91, 99, 121, 97, 109, 106, 102, 104, 107, 955.

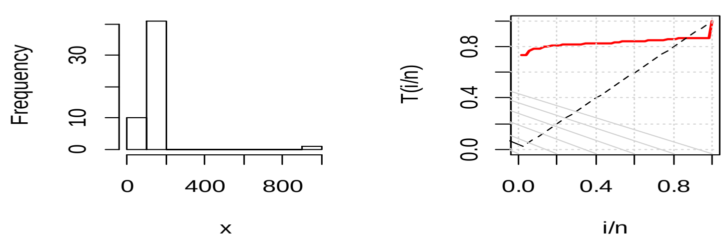

Figure 78. The IQ for 52 non-white males, hired by a large insurance company in 1971

79- The following symmetric data presented by [47], deals in the fatigue life of 6061-T6 aluminum coupons cut parallel to the direction of rolling and oscillated at 18 cycles per second. The data set consists of 101 observations with maximum stress per cycle 31,000 psi. The data are presented below (after subtracting 65 from each observation). The values are:

70, 90, 96, 97, 99, 100, 103, 104, 104, 105, 107, 108,108, 108, 109, 109, 112, 112 ,113, 114, 114, 114, 116, 119, 120, 120, 120, 121, 121, 123, 124, 124,124, 124, 124 ,128, 128, 129, 129, 130, 130, 130, 131, 131, 131, 131, 131, 132, 132, 132, 133, 134,134, 134, 134, 134, 136, 136, 137, 138, 138, 138, 139, 139, 141, 141, 142, 142, 142, 142, 142, 142, 144, 144, 145, 146, 148, 148, 149, 151, 151, 152, 155, 156, 157, 157, 157, 157, 158, 159, 162, 163, 163, 164, 166, 166, 168, 170, 174, 196, 212.

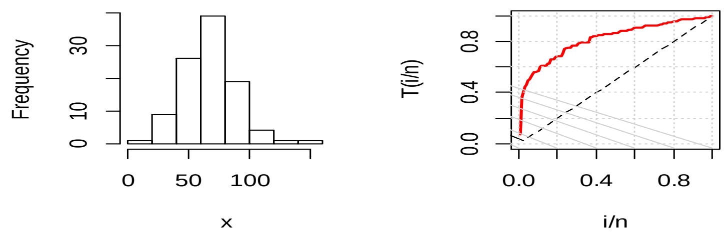

Figure 79. The symmetric of the fatigue life of 6061-T6 aluminum coupons

80- The following skewed to right natured a set of data is the survival times (in days) of 72 guinea pigs infected with virulent tubercle bacilli, reported by [48], The values are:

12, 15, 22, 24, 24, 32, 32, 33, 34, 38, 38, 43, 44, 48, 52, 53, 54, 54, 55, 56, 57, 58, 58, 59, 60, 60, 60, 60, 61, 62, 63, 65, 65, 67, 68, 70, 70, 72, 73, 75, 76, 76, 81, 83, 84, 85, 87, 91, 95, 96, 98, 99, 109, 110, 121, 127, 129, 131, 143, 146, 146, 175, 175, 211, 233, 258, 258, 263, 297, 341, 341, 376.

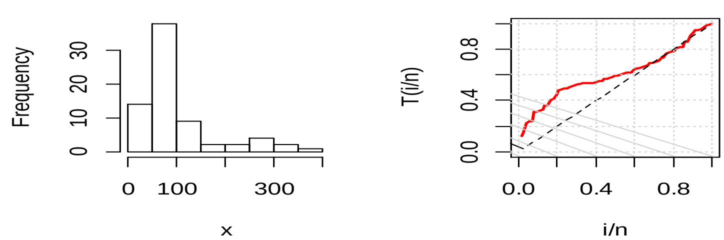

Figure 80. The skewed to right survival times of 72 guinea pigs infected with virulent tubercle bacilli

81- The following data set represented by [49], is the survival times of a group of patients suffering from Head and Neck cancer disease and treated using radiotherapy (RT). The observations of the extreme natured right skewed data is:

6.53, 7, 10.42, 14.48, 16.10, 22.70, 34, 41.55, 42, 45.28, 49.40, 53.62, 63, 64, 83, 84, 91, 108, 112, 129, 133, 133, 139, 140, 140, 146, 149, 154, 157, 160, 160, 165, 146, 149, 154, 157, 160, 160, 165, 173, 176, 218, 225, 241, 248, 273, 277, 297, 405, 417, 420, 440, 523, 583, 594, 1101, 1146, 1417.

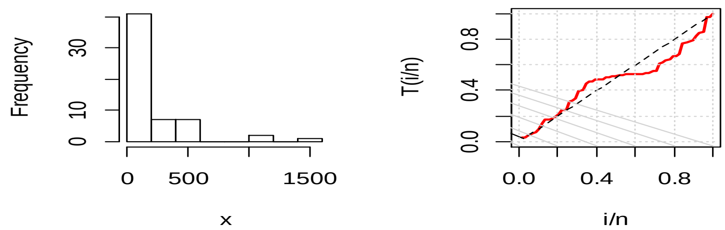

Figure 81. The survival times of a group of patients suffering from Head and Neck cancer disease

82- The following data presented by [50] is the vinyl chloride, obtains from clean up-gradient monitoring wells in mg/l. the observations of skewed to right data is given by:

5.1, 1.2, 1.3, 0.6, 0.5, 2.4, 0.5, 1.1, 8, 0.8, 0.4, 0.6, 0.9, 0.4, 2, 0.5, 5.3, 3.2, 2.7, 2.9, 2.5, 2.3, 1, 0.2, 0.1, 0.1, 1.8, 0.9, 2, 4, 6.8, 1.2, 0.4, 0.2.

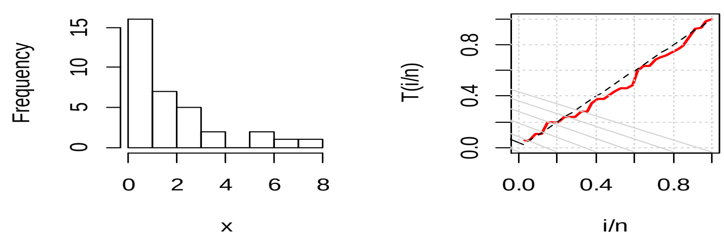

Figure 82. The vinyl chloride obtains from clean up-gradient monitoring wells

83- The following extreme natured (right-skewed) data reported by [51], is the times between successive failures of air conditioning equipment in a Boeing 720 airplane. The data set is:

74, 57, 48, 29, 502, 12, 70, 21, 29, 386, 59, 27, 153, 26, 326.

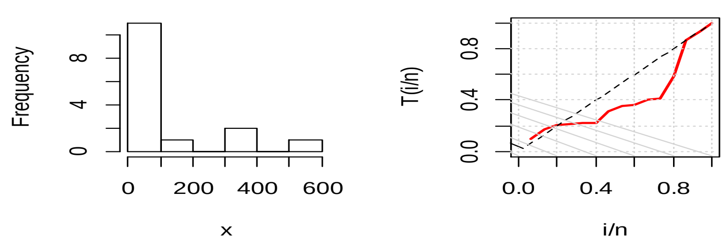

Figure 83. The right-skewed of the times between successive failures of air conditioning equipment

84- The following lifetime skewed to right natured data discussed by [52], is the relief times (in minutes) of 20 patients receiving an analgesic. The values are:

1.1, 1.4, 1.3, 1.7, 1.9, 1.8, 1.6, 2.2, 1.7, 2.7, 4.1, 1.8, 1.5, 1.2, 1.4, 3, 1.7, 2.3, 1.6, 2.

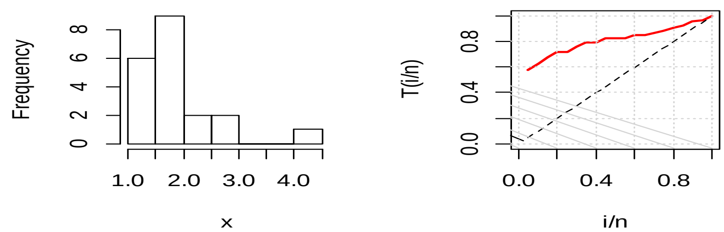

Figure 84. The lifetime skewed to the relief times of 20 patients receiving an analgesic

85- The following moderately skewed to right a set of data discussed by [53], is the glass strength of aircraft window. The values are:

18.83, 20.8, 21.657, 23.03, 23.23, 24.05, 24.321, 25.5, 25.52, 25.8, 26.69, 26.77, 26.78, 27.05, 27.67, 29.9, 31.11, 33.2, 33.73, 33.76, 33.89, 34.76, 35.75, 35.91, 36.98, 37.08, 37.09, 39.58, 44.045, 45.29, 45.381.

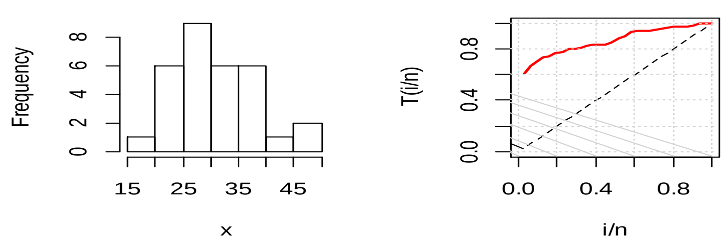

Figure 85. The moderately skewed to the glass strength of aircraft window

86- The following extreme natured (right skewed) data presented by [54], deals in the time between failures (thousands of hours) of secondary reactor pumps. The values are:

2.160, 0.746, 0.402, 0.954, 0.491, 6.560, 4.992, 0.347, 0.150, 0.358, 0.101, 1.359, 3.465, 1.060, 0.614, 1.921, 4.082, 0.199, 0.605, 0.273, 0.070, 0.062, 5.320.

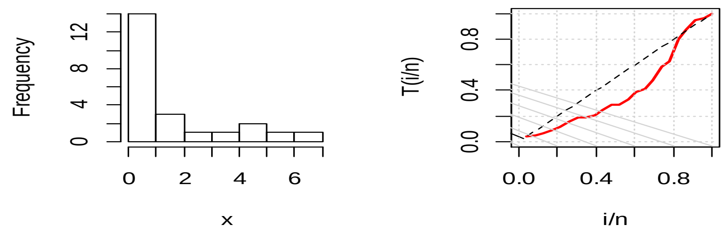

Figure 86. The right skewed to the time between failures of secondary reactor pumps

87- The following slightly skewed to the left, a set of data corresponds to fifty two ordered annual maximum antecedent rainfall measurements in millimeter (mm) from Maple Ridge in British Columbia, Canada, discussed by [55]. The values are:

264.9, 314.1, 364.6, 379.8, 419.3, 457.4, 459.4, 460, 490.3, 490.6, 502.2, 525.2, 526.8, 528.6, 528.6, 537.7, 539.6, 540.8, 551.0, 573.5, 579.2, 588.2, 588.7, 589.7, 592.1, 592.8, 600.8, 604.4, 608.4, 609.8, 619.2, 626.4, 629.4, 636.4, 645.2, 657.6, 663.5, 664.9, 671.7, 673.0, 682.6, 689.8, 698, 698.6, 698.8, 703.2, 755.9, 786, 787.2, 798.6, 850.4, 895.1.

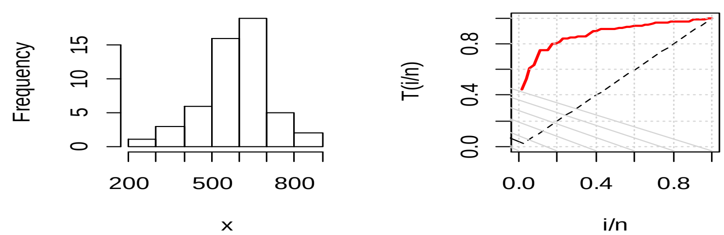

Figure 87. The skewed to fifty two ordered annual maximum antecedent rainfall measurements

88- The following extreme natured (right skewed) data presented by [56], relates to the length of intervals between times at which vehicles pass a point on a road. The values are:

2.5, 2.6, 2.6, 2.7, 2.8, 2.8, 2.9, 3,3, 3.1, 3.2, 3.4, 3.7, 3.9, 3.9, 3.9, 4.6, 4.7, 5, 5.6, 5.7, 6, 6, 6.1, 6.6, 6.9, 6.9, 7.3, 7.6, 7.9, 8, 8.3, 8.8, 9.3, 9.4, 9.5, 10.1, 11, 11.3, 11.9, 11.9, 12.3, 12.9, 12.9, 13, 13.8, 14.5, 14.9, 15.3, 15.4, 15.9, 16.2, 17.6, 20.1, 20.3, 20.6, 21.4, 22.8, 23.7, 23.7, 24.7, 29.7, 30.6, 31, 34.1, 34.7, 36.8, 40.1, 40.2, 41.3, 42, 44.8, 49.8, 51.7, 55.7, 56.5, 58.1, 70.5, 72.6, 87.1, 88.6, 91.7, 119.8.

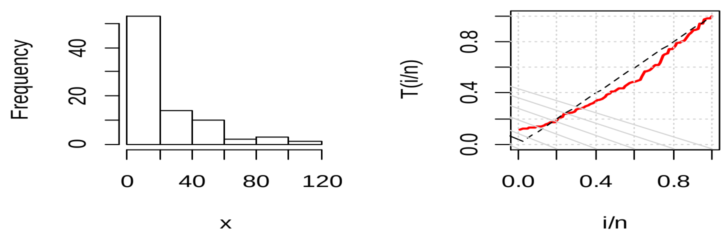

Figure 88. The right skewed to the length of intervals between times at which vehicles pass a point on a road

89- The following moderately right skewed a set data discussed by [57], consists of Stream flow amounts (1000 acre-feet) for 35 year (1936-70) at the U.S. Geological Survey (USGS) gagging station number 9-3425 for April 1-August 31 of each year and the observation are: 192.48, 303.91, 301.26, 135.87, 126.52, 474.25, 297.17, 196.47, 327.64, 261.34, 96.26, 160.52, 314.60, 346.30, 154.44, 111.16, 389.92, 157.93, 126.46, 128.58, 155.62, 400.93, 248.57, 91.27, 238.71, 140.76, 228.28, 104.75, 125.29, 366.22, 192.01, 149.74, 224.58, 242.19, 151.25.

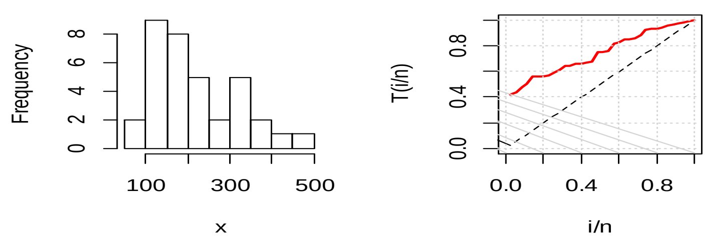

Figure 89. The right-skewed Stream flow amounts for 35 years in the U.S.

90- The following data approaches to symmetric behavior, presents the fatigue life (rounded to the nearest thousand cycles) for 67 specimens of Alloy T7987 that failed before having accumulated 300 thousand cycles of testing discussed by [32]. The observations are: 94, 118, 139, 159, 171, 189, 227, 96, 121, 140, 159, 172, 190, 256, 99, 121, 141, 159, 173, 196, 257, 99, 123, 141, 159, 176, 197, 269, 104, 129, 143, 162, 177, 203, 271, 108, 131, 144, 168, 180, 205, 274, 112, 133, 149, 168, 180, 211, 291, 114, 135, 149, 169, 184, 213, 117, 136, 152, 170, 187, 224, 117, 139, 153, 170, 188, 226.

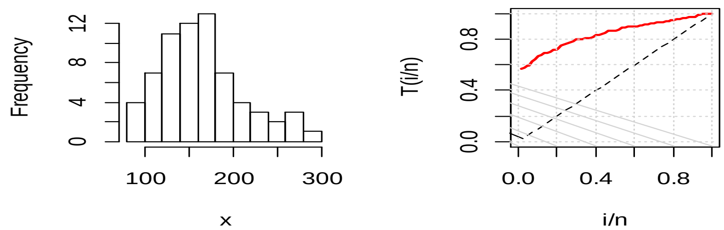

Figure 90. The symmetric behavior for 67 specimens of Alloy T7987

91- The following skewed to right, a set of data discussed by [58], details about the daily ozone measurements in New York, May-September1973. The observations are:

41, 36, 12, 18, 28, 23, 19, 8,7,16, 11, 14, 18, 14, 34, 6, 30, 11, 1, 11, 4, 32, 23, 45, 115, 37, 29, 71, 39, 23, 21, 37, 20, 12, 13, 135, 49, 32, 64, 40, 77, 97, 97, 85, 10, 27, 7, 48, 35, 61, 79, 63, 16, 80, 108, 20, 52, 82, 50, 64, 59, 39, 9, 16, 78, 35, 66, 122, 89, 110, 44, 28, 65, 22, 59, 23, 31, 44, 21, 9,45, 168, 73, 76, 118, 84, 85, 96, 78, 73, 91, 47, 32, 20, 23, 21, 24, 44, 21, 28, 9, 13, 46, 18, 13, 24, 16, 13, 23, 36, 7, 14, 30, 14, 18, 20.

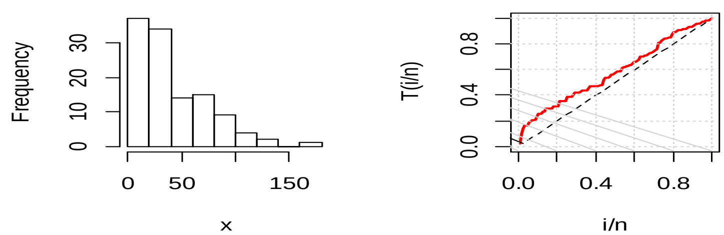

Figure 91. The skewed to right to the daily ozone measurements in New York

92- The following skewed to right a set of data is related to the study of total monthly rainfall during September at Sao Carlos located in southeastern Brazil discussed by [59]. Such a city has active industrial parole and high agricultural importance where the study of the behavior of dry and wet periods has proved to be strategic and economically significant in its development. The observation are:

26.40, 12.50, 1.00, 44.80, 0.00, 74.20, 179.50, 76.70, 269.50, 49.00, 306.80, 102.70, 73.50, 35.20, 72.70, 28.80, 49.30, 132.00, 151.50, 39.70, 136.20, 112.00, 17.70, 11.60, 225.20, 102.60, 27.10, 17.50, 6.70, 82.20, 40.70, 54.60, 115.50, 89.50, 0.00, 17.00, 127.40, 41.70, 43.10, 84.70, 102.50, 120.90, 80.10, 18.10, 5.30, 59.50, 26.80, 0.00, 34.30, 101.10, 60.30, 31.50, 60.40, 45.30, 49.50, 70.44.

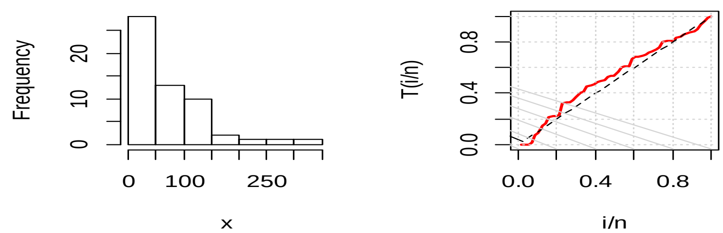

Figure 92. The skewed to the right of total monthly rainfall during September at Sao Carlos

93- The following bimodal set of data consists of 346 nicotine measurements made from several brands of cigarettes in 1998 see [60]. The data has been collected by the Federal Trade Commission which is an independent agency of the US government, whose main mission is the promotion of consumer protection. The observation are:

1.3, 1.0, 1.2, 0.9, 1.1, 0.8, 0.5, 1.0, 0.7, 0.5, 1.7, 1.1, 0.8, 0.5, 1.2, 0.8, 1.1, 0.9, 1.2, 0.9, 0.8, 0.6, 0.3, 0.8, 0.6, 0.4, 1.1, 1.1, 0.2, 0.8, 0.5, 1.1, 0.1, 0.8, 1.7, 1.0, 0.8, 1.0, 0.8, 1.0, 0.2, 0.8, 0.4, 1.0, 0.2, 0.8, 1.4, 0.8, 0.5, 1.1, 0.9, 1.3, 0.9, 0.4, 1.4, 0.9, 0.5, 1.7, 0.9, 0.8, 0.8, 1.2, 0.9, 0.8, 0.5, 1.0, 0.6, 0.1, 0.2, 0.5, 0.1, 0.1, 0.9, 0.6, 0.9, 0.6, 1.2, 1.5, 1.1, 1.4, 1.2, 1.7, 1.4, 1.0, 0.7, 0.4, 0.9, 0.7, 0.8, 0.7, 0.4, 0.9, 0.6, 0.4, 1.2, 2.0, 0.7, 0.5, 0.9, 0.5, 0.9, 0.7, 0.9, 0.7, 0.4, 1.0, 0.7, 0.9, 0.7, 0.5, 1.3, 0.9, 0.8, 1.0, 0.7, 0.7, 0.6, 0.8, 1.1, 0.9, 0.9, 0.8, 0.8, 0.7, 0.7, 0.4, 0.5, 0.4, 0.9, 0.9, 0.7, 1.0, 1.0, 0.7, 1.3, 1.0, 1.1, 1.1, 0.9, 1.1, 0.8, 1.0, 0.7, 1.6, 0.8, 0.6, 0.8, 0.6, 1.2, 0.9, 0.6, 0.8, 1.0, 0.5, 0.8, 1.0, 1.1, 0.8, 0.8, 0.5, 1.1, 0.8, 0.9, 1.1, 0.8, 1.2, 1.1, 1.2, 1.1, 1.2, 0.2, 0.5, 0.7, 0.2, 0.5, 0.6, 0.1, 0.4, 0.6, 0.2, 0.5, 1.1, 0.8, 0.6, 1.1, 0.9, 0.6, 0.3, 0.9, 0.8, 0.8, 0.6, 0.4, 1.2, 1.3, 1.0, 0.6, 1.2, 0.9, 1.2, 0.9, 0.5, 0.8, 1.0, 0.7, 0.9, 1.0, 0.1, 0.2, 0.1, 0.1, 1.1, 1.0, 1.1, 0.7, 1.1, 0.7, 1.8, 1.2, 0.9, 1.7, 1.2, 1.3, 1.2, 0.9, 0.7, 0.7, 1.2, 1.0, 0.9, 1.6, 0.8, 0.8, 1.1, 1.1, 0.8, 0.6, 1.0, 0.8, 1.1, 0.8, 0.5, 1.5, 1.1, 0.8, 0.6, 1.1, 0.8, 1.1, 0.8, 1.5, 1.1, 0.8, 0.4, 1.0, 0.8, 1.4, 0.9, 0.9, 1.0, 0.9, 1.3, 0.8, 1.0, 0.5, 1.0, 0.7, 0.5, 1.4, 1.2, 0.9, 1.1, 0.9, 1.1, 1.0, 0.9, 1.2, 0.9, 1.2, 0.9, 0.5, 0.9, 0.7, 0.3, 1.0, 0.6, 1.0, 0.9, 1.0, 1.1, 0.8, 0.5, 1.1, 0.8, 1.2, 0.8, 0.5, 1.5, 1.5, 1.0, 0.8, 1.0, 0.5, 1.7, 0.3, 0.6, 0.6, 0.4, 0.5, 0.5, 0.7, 0.4, 0.5, 0.8, 0.5, 1.3, 0.9, 1.3, 0.9, 0.5, 1.2, 0.9, 1.1, 0.9, 0.5, 0.7, 0.5, 1.1, 1.1, 0.5, 0.8, 0.6, 1.2, 0.8, 0.4, 1.3, 0.8, 0.5, 1.2, 0.7, 0.5, 0.9, 1.3, 0.8, 1.2, 0.9.

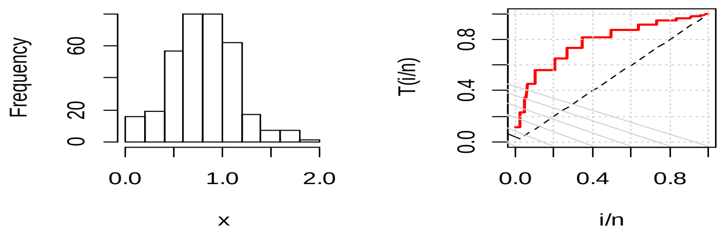

Figure 93. Bimodal of 346 nicotine measurements made from several brands of cigarettes

94- Generally it is observed that the brake pads of vehicles have a nominal lifetime, which is the number of miles or kilometers driven before the pads are reduced to a specified minimum thickness. To study the lifetime distribution, a manufacturer selected a random sample of 98 vehicles sold over the preceding 12 months to a group of dealers. Only cars that still had the initial pads were selected. For each car, the brake pad lifetime (x) could have then been observed by following the cars prospectively. The following moderately skewed to right a set of data explains the life times of 98 vehicles given by [31].

38.7, 49.2, 42.4, 73.8, 46.7, 44.1, 61.9, 39.3, 49.8, 46.3, 56.2, 50.5, 54.9, 54.0, 49.2, 44.8, 72.2, 107.8, 81.6, 45.2, 124.6, 64.0, 83.0, 143.6, 43.4, 69.6, 74.8, 32.9, 51.5, 31.8, 77.6, 63.7, 83.0, 24.8, 68.8, 68.8, 89.1, 65.0, 65.1, 59.3, 53.9, 79.4, 47.4, 61.4, 72.8, 54.0, 37.2, 44.2, 50.8, 65.5, 86.7, 43.8, 100.6, 67.6, 89.5, 60.3, 103.6, 82.6, 88.0, 42.4, 68.9, 95.7, 78.1, 83.6, 18.6, 92.6, 42.4, 34.3, 105.6, 20.8, 52.0, 77.2, 68.9, 78.7, 165.5,79.5, 55.0, 46.8, 124.5, 92.5, 110.0, 101.2, 59.4,27.8, 33.6, 69.0, 75.2, 58.4, 105.6, 56.2, 55.9, 83.8, 123.5,69.0, 101.9, 87.6, 38.8, 74.7.

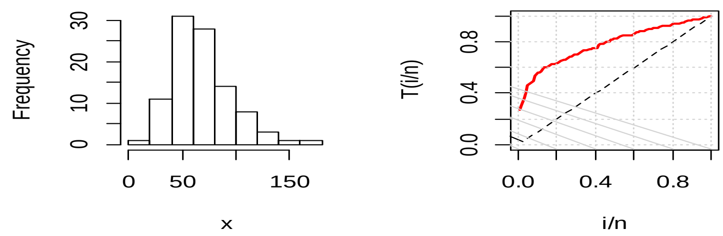

Figure 94. The brake pads of vehicles have a nominal lifetime

95- The following skewed to right a set of data reports the advanced lung cancer patients, taken from a study discussed by [31], who were randomly assigned the chemotherapy treatments termed as "standard". Survival times *t*, measured from the start of treatment for each patient. The data is:

411, 126, 118, 82, 8, 25, 11, 54, 153, 16, 56, 21, 287, 10, 8, 12, 177, 12, 200, 250, 100.

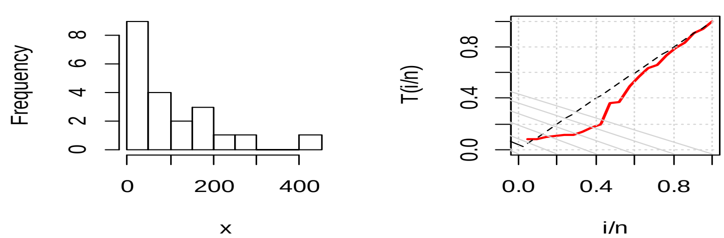

Figure 95. The skewed to the right set of data reports the advanced lung cancer patients

96- The following uncensored skewed to right a set of data shows that the 45 yearly survival times data of a group of patients who received only chemotherapy treatment. The data set was reported by [61].

0.047, 0.115, 0.121, 0.132, 0.164, 0.197, 0.203, 0.260, 0.282, 0.296, 0.334, 0.395, 0.458, 0.466, 0.501, 0.507, 0.529, 0.534, 0.540, 0.641, 0.644, 0.696, 0.841, 0.863, 1.099, 1.219, 1.271, 1.326, 1.447, 1.485, 1.553, 1.581, 1.589, 2.178, 2.343, 2.416, 2.444, 2.825, 2.830, 3.578, 3.658, 3.743, 3.978, 4.003, 4.033.

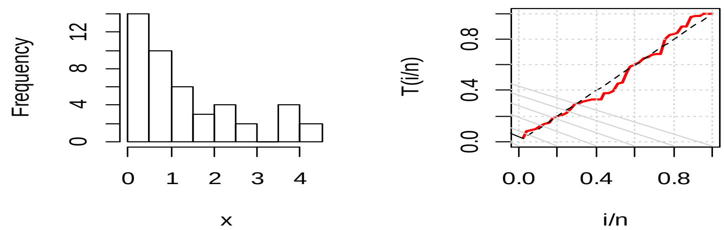

Figure 96. Uncensored skewed to the right of the 45 yearly survival times data of a group of patients

97- The following extreme (skewed to right) a set of data discussed by [31] present the number of cycles to failure for a group of 60 electrical appliances in a life test. The failure times have been ordered for convenience.

14, 34, 59, 61, 69, 80, 123, 142, 165, 210, 381, 464, 479, 556, 574, 839, 917, 969, 991, 1064, 1088, 1091, 1174, 1270, 1275, 1355, 1397, 1477, 1578, 1649, 702, 1893, 1932, 2001, 2161, 2292, 2326 , 2337, 2628, 2785, 2811, 2886, 2993, 3122, 3248, 3715, 3790, 3857, 3912, 4100, 410, 4116, 4315, 4510, 4584, 5267, 5299, 5583, 6065, 9701.

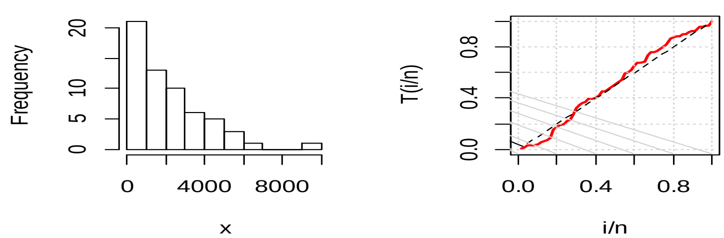

Figure 97. The skewed to right to the number of cycles to failure for a group of 60 electrical appliances

98- The following moderately skewed to right a set of data analyzed by [62], covers the annual maximum daily precipitation in millimeter record in Basan, Korea, from 1904 to 2011.The observations are:

24.8, 140.9, 54.1, 153.5, 47.9, 165.5, 68.5, 153.1, 254.7, 175.3, 87.6, 150.6, 147.9, 354.7, 128.5, 150.4, 119.2, 69.7, 185.1, 153.4, 121.7, 99.3, 126.9, 150.1, 149.1, 143, 125.2, 97.2, 179.3, 125.8, 101, 89.8, 54.6, 283.9, 94.3, 165.4, 48.3, 69.2, 147.1, 114.2, 159.4, 114.9, 58.5, 76.6, 20.7, 107.1, 244.5, 126, 122.2, 219.9, 153.2, 145.3, 101.9, 135.3, 103.1, 74.7, 174, 126, 144.9, 226.3, 96.2, 149.3, 122.3, 164.8, 188.6, 273.2, 61.2, 84.3, 130.5, 96.2, 155.8, 194.6, 92, 131, 137, 106.8, 131.6, 268.2, 124.5, 147.8, 294.6, 101.6, 103.1, 247.5, 140.2, 153.3, 91.8, 79.4, 149.2, 168.6, 127.7, 332.8, 261.6, 122.9, 273.4, 178, 177, 108.5, 115, 241, 76, 127.5, 190, 259.5, 301.5.

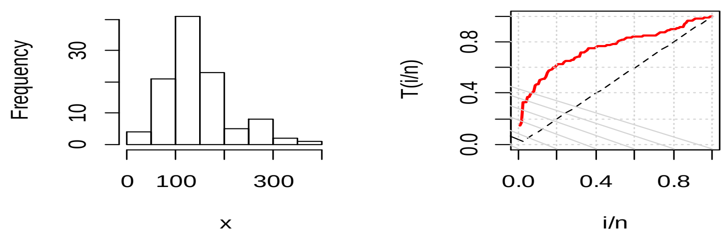

Figure 98. The moderately skewed to the right of covers the annual maximum daily precipitation

99- The following skewed to right a set of data developed by [63], relates to minimum monthly flows of water (m3/s) on the Piracicaba River, located in Sao Paulo state, Brazil. This study can be useful to protect and maintain aquatic resources for the state. This data set is obtained from the Department of Water Resources and Power agency manager of water resources of the State of Sao Paulo from 1960 to 2014. The data set is:

***FOR MAY*:** 29.19, 18.47, 12.86, 151.11, 19.46, 19.46, 84.30, 19.30, 18.47, 34.12, 374.54, 19.72, 25.58, 45.74, 68.53, 36.04, 15.92, 21.89, 40.00, 44.10, 33.35, 35.49, 56.25, 24.29, 23.56, 50.85, 24.53, 13.74, 27.99, 59.27, 13.31, 41.63, 10.00, 33.62, 32.90, 27.55, 16.76, 47.00, 106.33, 21.03.

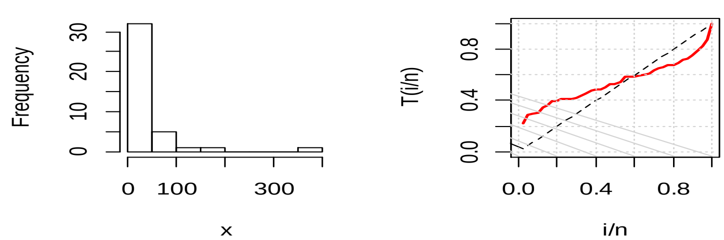

Figure 99. The right skewed a set of data to minimum monthly flows of water on the Piracicaba River FOR MAY

FOR JUNE: 13.64, 39.32, 10.66, 224.07, 40.90, 22.22, 14.44, 23.59, 47.02, 37.01, 432.11, 10.63, 28.51, 11.77, 25.35, 25.80, 39.73, 9.21, 22.36, 11.63, 33.35, 18.00, 18.62, 17.71, 100.10, 23.32, 11.63, 10.20, 12.04, 11.63, 50.57, 11.63, 33.72, 14.69, 12.30, 32.90, 179.75, 37.57, 7.95.

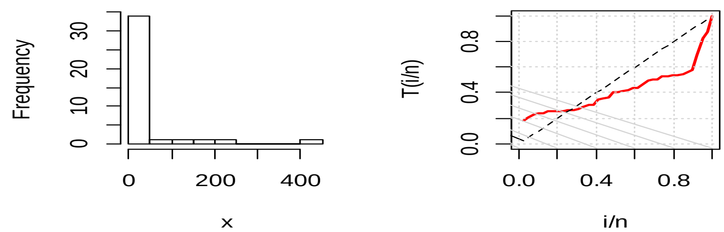

Figure 100. The right skewed a set of data to minimum monthly flows of water on the Piracicaba River FOR JUNE

FOR JULY: 12.98, 15.66, 13.18, 174.94, 10.35, 47.52, 13.28, 24.03, 11.40, 22.71, 43.96, 9.38, 11.40, 13.28, 14.84, 14.44, 63.74, 12.04, 17.26, 28.74, 12.25, 10.22, 26.25, 13.31, 28.24, 12.88, 17.71, 8.82, 10.40, 7.67, 49.15, 17.93, 9.80, 105.88, 10.77, 13.49, 19.77, 34.22, 7.26.

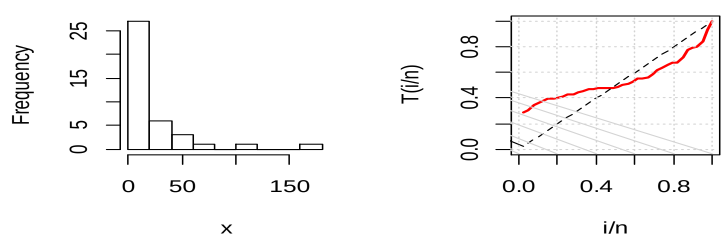

Figure 101. The right skewed a set of data to minimum monthly flows of water on the Piracicaba River FOR JULY

FOR AUGUST: 16.00, 9.52, 9.43, 53.72, 17.10, 8.52, 10.00, 15.23, 8.78, 28.97, 28.06, 18.26, 9.69, 51.43, 10.96, 13.74, 20.01, 10.00, 12.46, 10.40, 26.99, 7.72, 11.84, 18.39, 11.22, 13.10, 16.58, 12.46, 58.98, 7.11, 11.63, 8.24, 9.80, 15.51, 37.86, 30.20, 8.93, 14.29, 12.98, 12.01, 6.80.

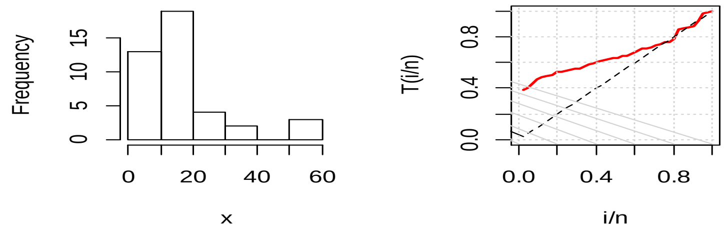

Figure 102. The right skewed a set of data to minimum monthly flows of water on the Piracicaba River FOR AUGUST

FOR SEPTEMBER: 29.19, 8.49, 7.37, 82.93, 44.18, 13.82, 22.28, 28.06, 6.84, 12.14, 153.78, 17.04, 13.47, 15.43, 30.36, 6.91, 22.12, 35.45, 44.66, 95.81, 6.18, 10.00, 58.39, 24.05, 17.03, 38.65, 47.17, 27.99, 11.84, 9.60, 6.72, 13.74, 14.60, 9.65, 10.39, 60.14, 15.51, 14.69, 16.44.

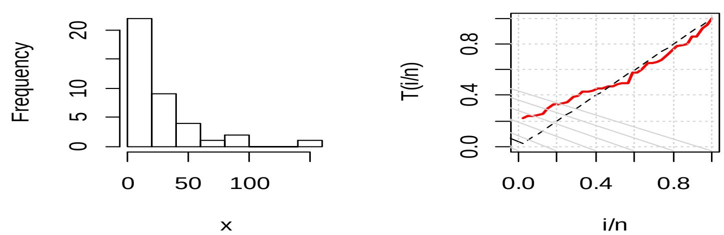

Figure 103. The skewed to right a set of data to minimum monthly flows of water on the Piracicaba River FOR SEPTEMBER

100- The following symmetric a set of data is related to a civil engineering with 85 hailing times discussed by [64]. The values are:

4.79, 4.75, 5.40, 4.70, 6.50, 5.30, 6.00, 5.90, 4.80, 6.70, 6.00, 4.95, 7.90, 5.40, 3.50, 4.54, 6.90, 5.80, 5.40, 5.70, 8.00, 5.40, 5.60, 7.50, 7.00, 4.60, 3.20, 3.90, 5.90, 3.40, 5.20, 5.90, 4.40, 5.20, 7.40, 5.70, 6.00, 3.60, 6.20, 5.70, 5.80, 5.90, 6.00, 5.15, 6.00, 4.82, 5.90, 6.00, 7.30, 7.10, 4.73, 5.90, 3.60, 6.30, 7.00, 5.10, 6.00, 6.60, 4.40, 6.80, 5.60, 5.90, 5.90, 8.60, 6.00, 5.80, 5.40, 6.50, 4.80, 6.40, 4.15, 4.90, 6.50, 8.20, 7.00, 8.50, 5.90, 4.40, 5.80, 4.30, 5.10, 5.90, 4.70, 3.50, 6.80.

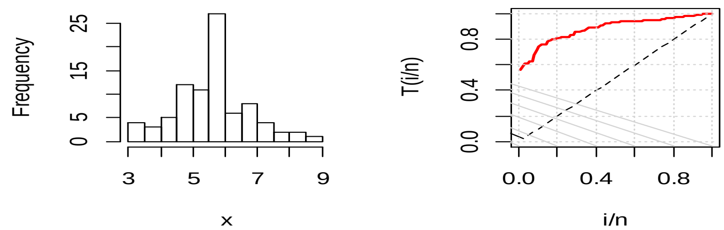

Figure 104. The symmetric a set of data is related to a civil engineering with 85 hailing times

101- The following moderately skewed to right a set of data used by [65] represents the permeability the ability of a substance to allow gases or liquids_to go through it values from three horizons of the Dominquez field of Southern California. Permeability data measured in militaries (a unit of porous permeability equal to 1/1000 darcy) are:

292, 346, 403, 640, 191, 353, 447, 696, 251, 390, 498, 615, 248, 370, 424, 650, 241, 370, 523, 799, 203, 305, 585, 707, 294, 497, 565, 832, 217, 402, 558, 810, 214, 484, 530, 888, 282, 439, 539, 883, 299, 425, 568, 824, 370, 466, 625, 975, 320, 477, 680, 937, 377, 426, 660.

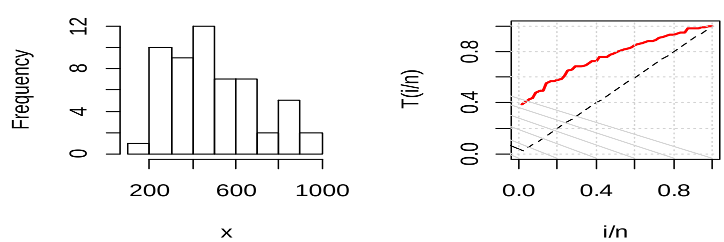

Figure 105. The moderately skewed to right of the permeability the ability of a substance

102- The following skewed to right a set of data relates to the sports and can be downloaded directly from www.stat.auckland.ac.nz/~lee/330/datasets.dir/sport. data and the observations are:

19.75, 21.30, 19.88, 23.66, 17.64, 15.58, 19.99, 22.43, 17.95, 15.07, 28.83, 18.08, 23.30, 17.71, 18.77, 19.83, 25.16, 18.04, 21.79, 22.25, 16.25, 16.38, 19.35, 19.20, 17.89, 12.20, 23.70, 24.69, 16.58, 21.47, 20.12, 17.51, 23.70, 22.39, 20.43, 11.29, 25.26, 19.39, 19.63, 23.11, 16.86, 21.32, 26.57, 17.93, 24.97, 22.62, 15.01, 18.14, 26.78, 17.22, 26.50, 23.01, 30.10, 13.93, 26.65, 35.52, 15.59, 19.61, 14.52, 11.47, 17.71, 18.48, 11.22, 13.61, 12.78, 11.85, 13.35, 11.77, 11.07, 21.30, 20.10, 24.88, 19.26, 19.51, 23.01, 8.07, 11.05, 12.39, 15.95, 9.91, 16.20, 9.02, 14.26, 10.48, 11.64, 12.16, 10.53, 10.15, 10.74, 20.86, 19.64, 17.07, 15.31, 11.07, 12.92, 8.45, 10.16, 12.55, 9.10, 13.46, 8.47, 7.68, 6.16, 8.56, 6.86, 9.40, 9.17, 8.54, 9.20, 11.72, 8.44, 7.19, 6.46, 9.00, 12.61, 9.03, 6.96, 10.05, 9.56, 9.36, 10.81, 8.61, 9.53, 7.42, 9.79, 8.97, 7.49, 11.95, 7.35, 7.16, 8.77, 9.56, 14.53, 8.51, 10.64, 7.06, 8.87, 7.88, 9.20, 7.19, 6.06, 5.63, 6.59, 9.50, 13.97, 11.66, 6.43, 6.99, 6.00, 6.56, 6.03, 6.33, 6.82, 6.20, 5.93, 5.80, 6.56, 6.76, 7.22, 8.51, 7.72, 19.94, 13.91, 6.10, 7.52, 9.56, 6.06, 7.35, 6.00, 6.92, 6.33, 5.90, 8.84, 8.94, 6.53, 9.40, 8.18, 17.41, 18.08, 9.86, 7.29, 18.72, 10.12, 19.17, 17.24, 9.89, 13.06, 8.84, 8.87, 14.69, 8.64, 14.98, 7.82, 8.97, 11.63, 13.49, 10.25, 11.79, 10.05, 8.51, 11.50, 6.26.

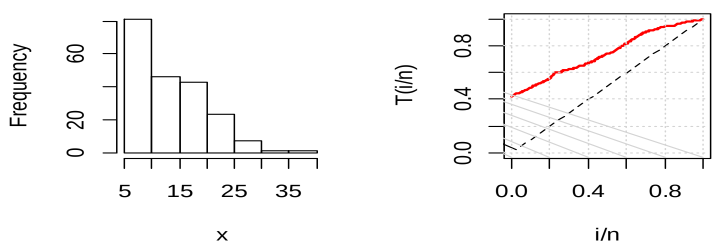

Figure 106. The skewed to right a set of data relates to the sports

103- The following skewed to right as set of data contains 61 observed recidivism failure times (in days) revealed by correctional institutions in Columbia USA, studied by [66]. The observations are:

1, 6, 9, 29, 30, 34, 39, 41, 44, 45, 49, 56, 84, 89, 91, 100, 103, 104, 115, 119, 124, 138, 141, 146, 156, 162, 168, 183, 185, 198, 209, 217, 217, 228, 233, 238, 241, 252, 258, 271, 275, 276, 279, 282, 305, 313, 329, 331, 334, 336,336, 362, 384, 404, 408, 422, 438, 441, 465, 486, 556.

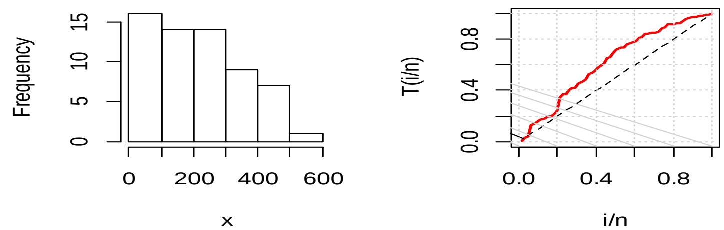

Figure 107. The skewed to right as set of data contains 61 observed recidivism failure times

104- The following skewed to left a set of data, presents the time between successive failures (in hours) of load-haul-dump machines for loading rock in underground mines is gathered and studied by [67]. The data is:

16, 39, 71, 95, 98, 110, 114, 226, 294, 344, 555, 599, 757, 822, 963, 1077, 1167, 1202, 1257, 1317, 1345, 1372, 1402, 1536, 1625, 1643, 1675, 1726, 1736, 1772, 1796, 1799, 1814, 1868, 1894, 1970, 2042, 2044, 2094, 2127, 2291, 2295, 2299, 2317.

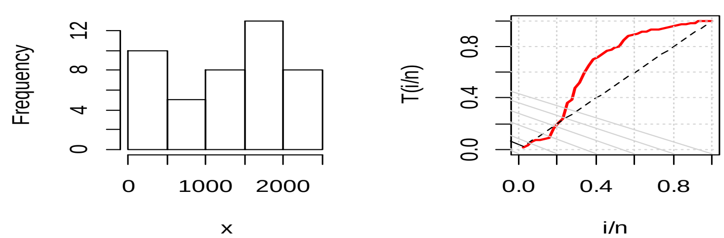

Figure 108. The skewed to left to the time between successive failures of load-haul-dump machines

105- The following symmetric set of a data consists of fracture toughness from the silicon nitride. The data can be downloaded directly from the web-site http://www.ceramics.nist.gov/srd/summary/ftmain.htm and also studied by [25]. The data is:

5.50, 5.00, 4.90, 6.40, 5.10, 5.20, 5.20, 5.00, 4.70, 4.00, 4.50, 4.20, 4.10, 4.56, 5.01, 4.70, 3.13, 3.12, 2.68, 2.77, 2.70, 2.36, 4.38, 5.73, 4.35, 6.81, 1.91, 2.66, 2.61, 1.68, 2.04, 2.08, 2.13, 3.80, 3.73, 3.71, 3.28, 3.90, 4.00, 3.80, 4.10, 3.90, 4.05, 4.00, 3.95, 4.00, 4.50, 4.50, 4.20, 4.55, 4.65, 4.10, 4.25, 4.30, 4.50, 4.70, 5.15, 4.30, 4.50, 4.90, 5.00, 5.35, 5.15, 5.25, 5.80, 5.85, 5.90, 5.75, 6.25, 6.05, 5.90, 3.60, 4.10, 4.50, 5.30, 4.85, 5.30, 5.45, 5.10, 5.30, 5.20, 5.30, 5.25, 4.75, 4.50, 4.20, 4.00, 4.15, 4.25, 4.30, 3.75, 3.95, 3.51, 4.13, 5.40, 5.00, 2.10, 4.60, 3.20, 2.50, 4.10, 3.50, 3.20, 3.30, 4.60, 4.30, 4.30, 4.50, 5.50, 4.60, 4.90, 4.30, 3.00, 3.40, 3.70, 4.40, 4.90, 4.90, 5.00.

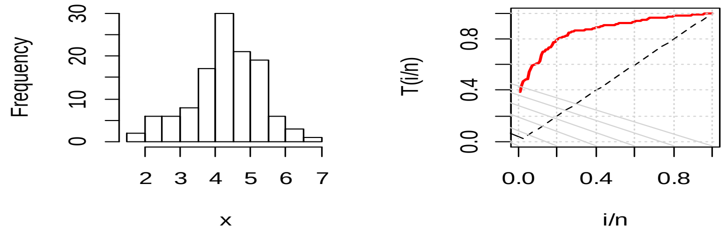

Figure 109. The symmetric set of fracture toughness from the silicon nitride

106- The following skewed to right a real time set of data is obtained from the R base package [68]. The data consists of plasma concentrations of indomethacin (mcg/ml). The observations are:

1.50, 0.94, 0.78, 0.48, 0.37, 0.19, 0.12, 0.11, 0.08, 0.07, 0.05, 2.03, 1.63, 0.71, 0.70, 0.64, 0.36, 0.32, 0.20, 0.25, 0.12, 0.08, 2.72, 1.49, 1.16, 0.80, 0.80, 0.39, 0.22, 0.12, 0.11, 0.08, 0.08, 1.85, 1.39, 1.02, 0.89, 0.59, 0.40, 0.16, 0.11, 0.10, 0.07, 0.07, 2.05, 1.04, 0.81, 0.39, 0.30, 0.23, 0.13, 0.11, 0.08, 0.10, 0.06, 2.31, 1.44, 1.03, 0.84, 0.64, 0.42, 0.24, 0.17, 0.13, 0.10, 0.09.

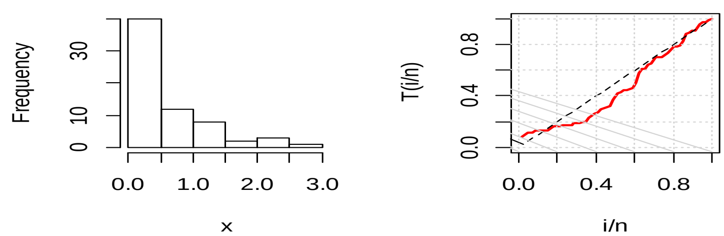

Figure 110. The skewed to right a real time set of data from the R base package

107- The following symmetric a set of data studied by [69], discusses the breaking strengths of 100 yarns given. The observations are:

66, 117, 132, 111, 107, 85, 89, 79, 91, 97, 138, 103, 111, 86, 78, 96, 93, 101, 102, 110, 95, 96, 88, 122, 115, 92, 137, 91, 84, 96, 97, 100, 105, 104, 137, 80, 104, 104, 106, 84, 92, 86, 104, 132, 94, 99, 102, 101, 104, 107, 99, 85, 95, 89, 102, 100, 98, 97, 104, 114, 111, 98, 99, 102, 91, 95, 111, 104, 97, 98, 102, 109, 88, 91, 103, 94, 105, 103, 96, 100, 101, 98, 97, 97, 101, 102, 98, 94, 100, 98, 99, 92, 102, 87, 99, 62, 92, 100, 96, 98.

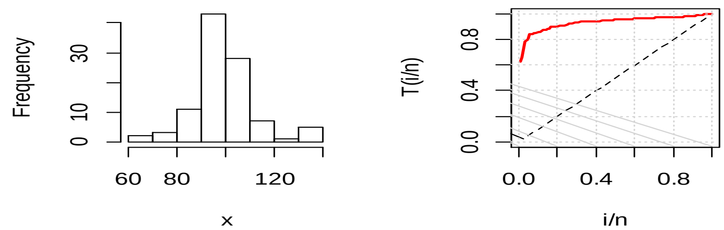

Figure 111. The symmetric set of data to the breaking strengths of 100 yarns

108- The following extreme (skewed to right) a set of data reported by [70], relates to the influence of physiographic (the systematic description of nature in general) and historical factors on species richness of native and non-native vascular plants on 22 coastal islands are selected. Different variables are affecting the richness. We select the variable area (hectares) having values:

3, 4, 4, 8, 10, 34, 40, 46, 47, 61, 128, 140, 350, 1190, 1350, 1900, 2300, 2707, 10900, 13600, 13600, 26668.

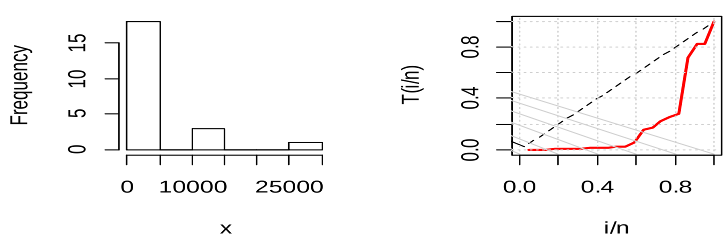

Figure 112. The skewed to right to the influence of physiographic and historical factors

109- The three real data of COVID-19 mortality rates from Italy, Mexico, and the Netherlands [see https://covid19.who.int/] discussed by [71]

***Italy*:** The first data represents a COVID-19 mortality rates data belongs to Italy of 59 days, that is recorded from 27 February to 27 April 2020. The data are as follows:

4.571, 7.201, 3.606, 8.479, 11.410, 8.961, 10.919, 10.908, 6.503, 18.474, 11.010, 17.337, 16.561, 13.226, 15.137, 8.697, 15.787, 13.333, 11.822, 14.242, 11.273, 14.330, 16.046, 11.950, 10.282, 11.775, 10.138, 9.037, 12.396, 10.644, 8.646, 8.905, 8.906, 7.407, 7.445, 7.214, 6.194, 4.640, 5.452, 5.073, 4.416, 4.859, 4.408, 4.639, 3.148, 4.040, 4.253, 4.011, 3.564, 3.827, 3.134, 2.780, 2.881, 3.341, 2.686, 2.814, 2.508, 2.450, 1.518.

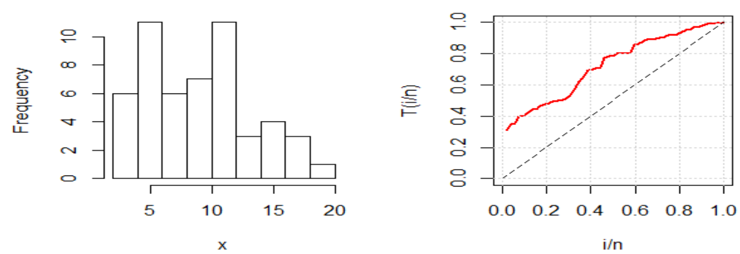

Figure 113. A bimodal to COVID-19 mortality rates from Italy form 27 February to 27 April 2020

Mexico: The second data represents a COVID-19 mortality rate data belongs to Mexico of 108 days that is recorded from 4 March to 20 July 2020. This data formed of rough mortality rate.

The data are as follows:

8.826, 6.105, 10.383, 7.267, 13.220, 6.015, 10.855, 6.122, 10.685, 10.035, 5.242, 7.630, 14.604, 7.903, 6.327, 9.391, 14.962, 4.730, 3.215, 16.498, 11.665, 9.284, 12.878, 6.656, 3.440, 5.854, 8.813, 10.043, 7.260, 5.985, 4.424, 4.344, 5.143, 9.935, 7.840, 9.550, 6.968, 6.370, 3.537, 3.286, 10.158,8.108, 6.697, 7.151, 6.560, 2.988, 3.336, 6.814, 8.325, 7.854, 8.551, 3.228, 3.499, 3.751, 7.486, 6.625, 6.140, 4.909, 4.661, 1.867, 2.838, 5.392, 12.042, 8.696, 6.412, 3.395, 1.815, 3.327, 5.406, 6.182,4.949, 4.089, 3.359, 2.070, 3.298, 5.317, 5.442, 4.557, 4.292, 2.500, 6.535, 4.648, 4.697, 5.459, 4.120, 3.922, 3.219, 1.402, 2.438, 3.257, 3.632, 3.233, 3.027, 2.352, 1.205, 2.077, 3.778, 3.218, 2.926, 2.601, 2.065, 1.041, 1.800, 3.029, 2.058, 2.326, 2.506, 1.923.

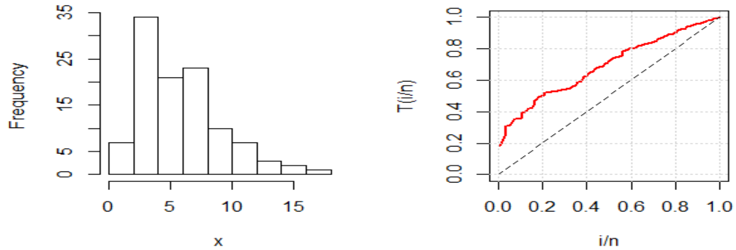

Figure 114. A right skewed to COVID-19 mortality rates from Mexico from 4 March to 20 July 2020

Netherlands: The third data represents a COVID-19 data belonging to the Netherlands of 30 days, which recorded from 31 March to 30 April 2020. This data formed of rough mortality rate. The data are as follows:

14.918, 10.656, 12.274, 10.289, 10.832, 7.099, 5.928, 13.211, 7.968, 7.584, 5.555, 6.027, 4.097, 3.611, 4.960, 7.498, 6.940, 5.307, 5.048, 2.857, 2.254, 5.431, 4.462, 3.883, 3.461, 3.647, 1.974, 1.273, 1.416, 4.235.

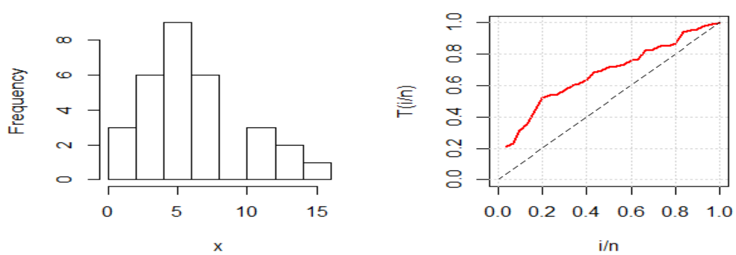

Figure 115. A right skewed to COVID-19 mortality rates from Netherlands from 31 March to 30 April 2020

110- The first data set presents the daily confirmed cases of COVID-19 in Pakistan from 24 March to 28 April 2020 (36 days) of COVID-19. First data set, is obtained from the following official electronic address: http://covid.gov.pk/stats/pakistan. The considered values are:

108, 102, 133, 170, 121, 99, 236, 178, 250, 161, 258, 172, 407, 577, 210, 243, 281, 186, 254, 336, 342, 269, 520, 414, 463, 514, 427, 796, 555, 742, 642, 785, 783, 605, 751, 806.

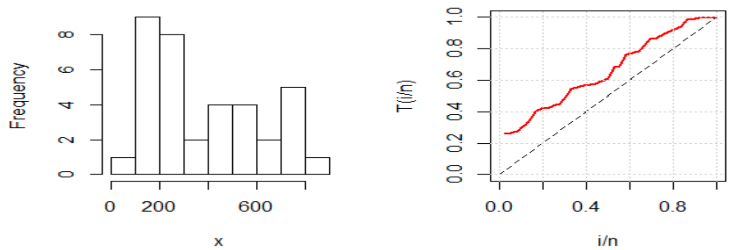

Figure 116. A right skewed to COVID-19 daily confirmed cases of COVID-19 in Pakistan from 24 March to 28 April 2020 (36 days)

The second data set, called COVID-19 data set II, has the same source, i.e., http://covid.gov.pk/stats/pakistan. It contains the daily recovered cases of COVID-19 in Pakistan from 24 March to 28 April 2020 (36 days). The considered values are given:

2, 2, 3, 4, 26, 24, 25, 19, 4, 40, 87, 172, 38, 105, 155, 35, 264, 69, 283, 68, 199, 120, 67, 36, 102, 96, 90, 181, 190, 228, 111, 163, 204, 192, 627, 263.

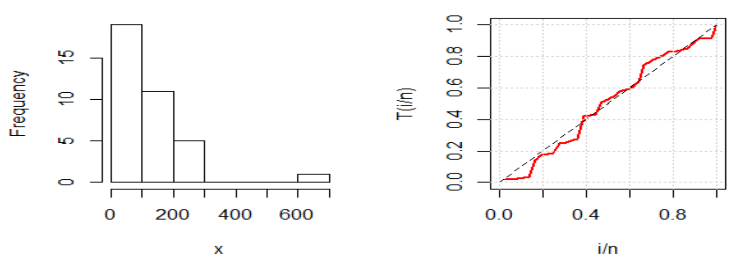

Figure 117. A right skewed to COVID-19 daily confirmed cases of COVID-19 in Pakistan from 24 March to 28 April 2020 (36 days)

111- The daily new COVID-19 confirmed cases in Pakistan from 21 March to 29 May 2020 (inclusive). The dataset was obtained from the following electronic address: http://covid.gov.pk/stats/ pakistan. It is given as follows:

112, 157, 89, 108, 102, 133, 170, 121, 99, 236, 178, 250, 161, 258, 172, 407, 577, 210, 243, 281, 186, 254, 336, 342, 269, 543, 488, 463, 514, 427, 796, 555, 742, 642, 785, 783, 605, 751, 806, 942, 990, 1297, 989, 1083, 1315, 1049, 1523, 1764, 1637, 1991, 1476, 1140, 2255, 1452, 1430, 1581, 1352, 1974, 1841, 1932, 2193, 2603, 1743, 2164, 1748, 1356, 1446, 2241, 2636, 2429.

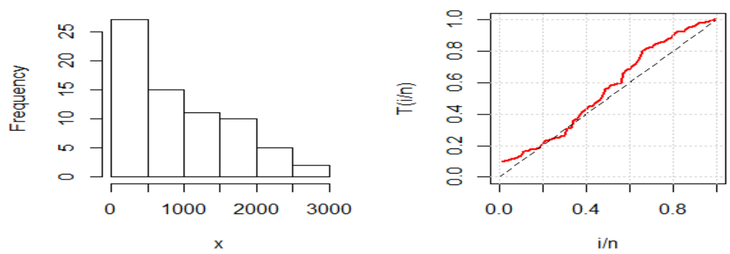

Figure 118. A right skewed to COVID-19 daily confirmed cases of COVID-19 in Pakistan from 21 March to 29 May 2020 (inclusive)

CONCLUSION

This comprehensive paper intended to discuss literature on the utility of datasets and to facilitate the practitioners of applied, theoretical as well as research scholars, whose research work is suffering owing to the unavailability of data. Accordingly, we pursued the International Impact Factor and Peer-Reviewed journals and books to acquire the multidisciplinary univariate continuous real-time datasets. As well, it was provided a solid foundation to the practitioners and researchers and they may continue their research work for the betterment of this world.

ACKNOWLEDGEMENT

The authors thank the referee for constructive comments.

CONFLICT OF INTERESTS

The authors declare that there is no conflict of interests.

REFERENCES

[1] M.V. Aarset, How to Identify a Bathtub Hazard Rate, IEEE Trans. Reliab. R-36 (1987), 106–108.

[2] V. Choulakian, M.A. Stephens, Goodness-of-Fit Tests for the Generalized Pareto Distribution, Technometrics. 43 (2001), 478–484.

[3] M.A.J. Van Montfort, On testing that the distribution of extremes is of type I when type II is the alternative, J. Hydrol. 11 (1970), 421–427.

[4] G. Kuczera, S. Frank, Australian rainfall Bruno book 3, Chapter 2: At-Site Flood Frequency Analysis-Draft, Engineers Australia, 10 March 2015.

[5] F.A. Bhatti, A. Ali, G.G. Hamedani, M. Ahmad, On the generalized log Burr III distribution: development, properties, characterizations and applications, Pak. J. Statist. 35 (2019), 25-51.

[6] R.V. Hogg, S.A. Klugman, Loss distributions, John Wiley & Sons, New York, (2009).

[7] J.F. Lawless, Statistical models and methods for lifetime data, John Wiley & Sons, New York, (1982).

[8] M.D. Nichols, W.J. Padgett, A Bootstrap Control Chart for Weibull Percentiles, Qual. Reliab. Eng. Int. 22 (2006), 141–151.

[9] R.L. Smith, J.C. Naylor, A Comparison of Maximum Likelihood and Bayesian Estimators for the Three-Parameter Weibull Distribution, Appl. Stat. 36 (1987), 358.

[10] E.T. Lee, J.W. Wang, Statistical methods for survival data analysis, Third ed. Wiley, New York, (2003).

[11] A.M. Abouammoh, S.A. Abdulghani, I.S. Qamber, On partial orderings and testing of new better than renewal used classes, Reliab. Eng. Syst. Safe. 43 (1994), 37–41.

[12] A.Z. Afify, Z.M. Nofal, N.S. Butt, Transmuted complementary Weibull geometric distribution, Pak. J. Stat. Oper. Res. 10 (2014), 435-454.

[13] E.T. Lee, Statistical methods for survival data analysis (2nd Edition), John Wiley and Sons Inc., New York, (1992).

[14] M. Smithson, J. Verkuilen, A better lemon-squeezer? Maximum likelihood regression with beta distributed dependent variables, Psychol. Meth. 11 (2006), 54-71.

[15] R. Dumonceaux, C.E. Antle, Discrimination between the log-normal and the weibull distributions, Technometrics. 15 (1973) 923–926.

[16] G.M. Cordeiro, R.D.S. Brito, The Beta Power distributions. Brazil. J. Probab. Stat. 26 (2012), 88-112.

[17] D.N.P. Murthy, M. Xie, R. Jiang, Weibull models, John Wiley & Sons Inc., Hoboken, (2004).

[18] J. Oliveira, J. Santos, C. Xavier, D. Trindade, G. M. Cordeiro, The McDonald half-logistic distribution: Theory and practice, Commun. Stat. Theory Meth. 45(7) (2013), 2005-2022.

[19] A.M. Nigm, E.K. AL-Hussaini, Z.F. Jaheen, Bayesian one sample prediction of future observations under Pareto distribution. Statistics, 37(6) (2003), 527-536.

[20] A.C. Frery, H.J. Muller, C.C.F. Yanasse, S.J.S. Sant'Anna, A model for extremely heterogeneous clutter. IEEE Trans. Geosci. Remote Sensing, 35(3) (1997), 648-659.

[21] G.M. Cordeiro, R.D.S. Brito, The beta power distributions. Brazil. J. Probab. Stat. 26(1) (2012), 88-112.

[22] R. Dasgupta, On the distribution of burr with applications, Sankhya B. 73 (2011), 1–19.

[23] M. Caramanis, J. Stremel, W. Fleck, S. Daniel, Probabilistic production costing: an investigation of alternative algorithms. Int. J. Electric. Power Energy Syst. 5(2) (1983), 75-86.

[24] D.H. Barlow, A.S. Cohen, M.T. Waddell, B.B. Vermilyea, J.S. Klosko, E.B. Blanchard, P.A. Di Nardo, Panic and generalized anxiety disorders: Nature and treatment, Behav. Therapy. 15 (1984), 431–449.

[25] S. Nadarajah, S. Kotz, On the alternative to the Weibull function. Eng. Frac. Mech. 74 (2007), 577-579.

[26] M.E. Ghitany, B. Atieh, S. Nadarajah, Lindley distribution and its application. Math. Computers Simul. 78 (2008), 493-506.

[27] M. Badar, A. Priest, Statistical Aspects of Fiber and Bundle Strength in Hybrid Composites. In: Hayashi, T., Kawata, S. and Umekawa, S., Eds., Progress in Science and Engineering Composites, ICCM-IV, Tokyo, (1982), 1129-1136.

[28] P. Feigl, M. Zelen, Estimation of exponential probabilities with concomitant information. Biometrics, 21 (1965), 826-838.

[29] G.S. Mudholkar, A.D. Hutson, The exponentiated Weibull family: Some properties and a flood data application, Commun. Stat. Theory Meth. 25(12) (1996), 3059-3083.

[30] D. Kundu, M.Z. Raqab, Estimation of $R = P(Y < X)$ for three-parameter Weibull distribution. Stat. Probab. Lett. 79(17) (2009), 1839-1846.

[31] J.F. Lawless, Statistical models and methods for lifetime data, 2nd Edition. John Wiley & Sons, Inc., Floboken, New Jersey, (2003).

[32] W.Q. Meeker, L.A. Escobar, Statistical methods for reliability data, Wiley, New York, (1998).

[33] K.B. Sylwia, Makeham's generalised distribution, Comput. Meth. Sci. Technol. 13 (2007), 113-120.

[34] M. Xie, Y. Tang, T.N. Goh, A modified Weibull extension with bathtub-shaped failure rate function, Reliab. Eng. Syst. Safe. 76(3) (2002), 279-285.

[35] K. Xu, M. Xie, L.C. Tang, S.L. Ho, Application of neural networks in forecasting engine systems reliability. Appl. Soft Comput. 2(4) (2003), 255-268.

[36] M.H. Tahir, G.M. Cordeiro, M. Mansoor, M. Zubair, The Weibull-Lomax distribution: properties and applications, Hacettepe J. Math. Stat. 44(2) (2015), 461-480.

[37] L.G. Pinho, G.M. Cordeiro, J.S. Nobre, The Harris extended exponential distribution. Commun. Stat. Theory Meth. 44 (2015), 3486-3502.

[38] B.A. Maguire, E. Pearson, A. Wynn, The time intervals between industrial accidents. Biometrika, 39(1952), 168-180.

[39] H. Linhart, W. Zucchini, The new probability distribution: an aspect to a life time distribution, model selection, Wiley & Sons, New York, (1986).

[40] M.M. Nassar, N.K. Nada, The beta generalized Pareto distribution. J. Stat., Adv. Theory Appl. 6 (2011), 1-17.

[41] D. Hinkley, On Quick Choice of Power Transformation, J. R. Stat. Soc., Ser. C (Appl. Stat.) 26 (1977), 67-69.

[42] M.E. Mead, On five-parameter lomax distribution: properties and applications. Pak. J. Stat. Oper. Res. 12(1) (2010), 185-199.

[43] M.A. Selim, Estimation and prediction for Nadarajah-Haghighi distribution based on record values. Pak. J. Stat. 34(1) (2018), 77-90.

[44] Z. Iqbal, M.M. Tahir, N. Riaz, et al. Generalized inverted kumaraswamy distribution: properties and application, Open J. Stat. 7 (2017), 645-662.

[45] R. Shanker, H. Fesshaye, S. Selvaraj, On modeling of lifetimes data using exponential and Lindley Distributions, Biometrics Biostat. Int. J. 2(5) (2015), 4-9.

[46] H.V. Roberts, Data analysis for managers with minitab. Scientific Press, Redwood City, CA, (1988).

[47] Z.W. Birnbaum, S.C. Saunders, Estimation for a family of life distributions with applications to fatigue. J. Appl. Probab. 6(2) (1969), 328-347.

[48] T. Bjerkedal, Acquisition of resistance in guinea pigs infected with different doses of virulent tubercle bacilli. Amer. J. Epidemiol. 72(1) (1960), 130–148.

[49] B. Efron, Logistic regression, survival analysis and the Kaplan Meier curve, J. Amer. Stat. Assoc. 83(402) (1988), 414-425.

[50] D.K. Bhaumik, K. Kapur, R.D. Gibbons, Testing parameters of a gamma distribution for small samples, Technometrics, 51(3) (2009), 326-334.

[51] F. Proschan, Theoretical explanation of observed decreasing failure rate. Technometrics, 5(3) (1963), 375-383.

[52] A.J. Gross, V.A. Clark, Survival distributions: reliability applications in the biometrical sciences, John Wiley, New York, USA, (1975).

[53] E.R. Fuller, Jr., S.W. Freiman, J.B. Quinn, G.D. Quinn, W.C. Carter, Fracture mechanics approach to the design of glass aircraft windows: a case study, in: P. Klocek (Ed.), San Diego, CA, 1994: pp. 419–430.

[54] M.S. Suprawhardana, Prayoto, Sangadji, Total time on test plot analysis for mechanical components of the RSG-GAS reactor. Atom Indones, 25(2) (1999), 155-161.

[55] G. Chen, C. Bunce, W. Jiang, A new distribution for extreme value analysis. In: Proceedings of the International Conference on Computational Intelligence and Software Engineering, (2010), 1-4.

[56] B. Jorgensen, Statistical properties of the generalized inverse gaussian distribution, Springer-Verlag, Heidelberg, (1982).

[57] P.W. Mielke, E.S. Johnson, Three parameter Kappa distribution maximum likelihood estimations and likelihood ratio tests. Mon. Weather Rev. 101 (1973), 701-707.

[58] S. Nadarajah, A truncated inverted beta distribution with application to air pollution data, Stoch. Environ. Res. Risk Assess. 22 (2008), 285–289.

[59] H.S. Bakouch, S. Dey, P.L. Ramos, F. Louzada, Binomial-exponential 2 Distribution: Different Estimation Methods and Weather Applications, Tend. Mat. Apl. Comput. (TEMA), 18 (2017), 0233.

[60] http: //www.ftc.gov/ reports/tobacco or http: // pw1.netcom.com/ rdavis2/ smoke. html.

[61] A. Bekker, J.J.J. Roux, P.J. Mosteit, A generalization of the compound Rayleigh distribution: using a Bayesian method on cancer survival times, Commun. Stat.-Theory Meth. 29(7) (2000), 1419-1433.

[62] B.Y. Jeong, Y.A. Seo, M.S. Murshed, J.S. Park, A three-parameter kappa distribution with hydrologic application: a generalized Gumbel distribution. Stochastic Environ. Res. Risk Assess. 28 (2014), 2063–2074.

[63] D.W. Reiser, T.A. Wesche, C. Estes, Status of instream flow legislation and practices in north America, Fisheries, 14(2) (1989), 22–29.

[64] S. Kotz, J. R. Dorp, Beyond beta: other continuous families of distributions with bounded support and applications, World Scientific Publishing Co., Singapore, (2004).

[65] K.L. Ricciardi, G.F. Pinder, K. Belitz, Comparison of the lognormal and beta distribution functions to describe the uncertainty in permeability. J. Hydrol. 313 (2005), 248-256.

[66] S. Stollmack, C.M. Harris, Failure-rate analysis applied to recidivism data. Oper. Res. 22 (1974), 1192-1205.

[67] U. Kumar, B. Klefsjo, S. Granholm, Reliability investigation for a fleet of load haul dump machines in a Swedish mine, Reliab. Eng. Syst. Safe. 26(4) (1989), 341-361.

[68] R.C. Team, R: a language and environment for statistical computing. Version 3.1. 2 [computer program]. R Foundation for Statistical Computing, Vienna, Austria, (2014).

[69] A.J. Duncan, Quality control and industrial statistics, Irwin Homewood, USA, (1974).

[70] S. Abbas, S.A. Taqi, F. Mustafa, et al. Topp-Leone inverse Weibull distribution: theory and application, Eur. J. Pure Appl. Math. 10(5) (2017), 1005-1022.

[71] H.M. Almongy, E.M. Almetwally, H.M. Aljohani, A.S. Alghamdi, E.H. Hafez, A new extended rayleigh distribution with applications of COVID-19 data, Results Phys. 23 (2021), 104012.